LOCAL HEAT FLUX IN A VERTICAL DUCT WITH

FREE CONVECTION IN OPPOSITION TO

FORCED FLOW

Contract #-nr-622 (01)

FINAL REPORT

Sponsored by

Office of Naval Research

31 December, 1959

DEPARTMENT OF CHEMICAL ENGINEERING

UNIVERSITY OF DELAWARE

NEWARK   DELAWARE

THIS REPORT HAS BEEN DELIMITED
AND CLEARED FOR PUBLIC RELEASE
UNDER DOD DIRECTIVE 5200.20 AND
NO RESTRICTIONS ARE IMPOSED UPON
ITS USE AND DISCLOSURE.

DISTRIBUTION STATEMENT A

APPROVED FOR PUBLIC RELEASE;
DISTRIBUTION UNLIMITED.

LOCAL HEAT FLUX IN A VERTICAL DUCT WITH
FREE CONVECTION IN OPPOSITION TO
FORCED FLOW

Contract #N-onr-622(01)

Sponsored by
Office of Naval Research

FINAL REPORT
31 December, 1952

Submitted by: S. A. Guerrieri, Assistant Professor
                      of Chemical Engineering

                Russell J. Hanna, Research Fellow in
                      Chemical Engineering

Department of Chemical Engineering
University of Delaware
Newark, Delaware

TABLE OF CONTENTS

LIST OF FIGURES

LIST OF TABLES

SUMMARY

Heat transfer rates accompanying simultaneous natural con-
vection and forced flow of air in a vertical channel, using an
optical method, were studied experimentally, under conditions
such that the two types of flow tended to oppose each other.
Thus the light, heated air tended to flow upward near the
vertical surfaces of the channel while the air stream as a
whole was forced to flow downward. These conditions are quali-
tatively similar to those occurring in cooling passages inside
blades of gas turbines.

Optical measurements showed that natural convective flow
predominated at low forced-flow velocities and high temperature
differences while at high mean velocities the flow was downward
even at the wall. Under intermediate conditions a maximum rate
of heat transfer occurred about half-way up the channel, owing
to instability of the laminar flow associated with the opposing
forces. At the highest mean velocities the local heat transfer
coefficients agreed closely with values expected from laminar-
flow theory neglecting natural convection.

INTRODUCTION

Two important types of fluid flow problems involving heat transfer are those of forced and those of free convection. Forced-convection flow is maintained either mechanically through a pressure drop or by means of hydrostatic head or by both. Free-convection flow, on the other hand, is caused by differences in the hydrostatic pressure of a fluid due to density differences because of temperature differences. Heat-transfer coefficients for the standard cases of forced and free convection are usually calculable by well known empirical and theoretical equations.

Flow produced by both free and forced convection forces simultaneously have now become of practical importance. Many aircraft propulsion systems contain components in which heat is being transferred. Free-convection flow due to density gradients is superimposed on the forced flow through helicopter ram jets and on the flow of air in the cooling passages in the blades of turbines. As will be seen, this can appreciably influence the resultant flow and heat transfer.

The present paper presents the mechanism and result of simultaneous action of forced and free convection forces on heat transfer when such forces are in direct opposition to each other. Data were taken in the range in which forced and free convection forces were of the same order of magnitude.

APPARATUS DESCRIPTION

The test unit was a vertical rectangular duct. Air was forced down through the duct while heat was supplied to two particular areas and caused a buoyant force in opposition to the pressure drop.

The sectional end view of Figure 2 shows the construction of the duct which can be considered to have been assembled in the following manner. Two machined and polished, rectangular, 1/2-inch aluminum plates, 8" x 12" formed the heating surface. These were held 1.01" apart, parallel and with the 12" axis vertical. Sides were put on these plates to form a vertical duct, open at both top and bottom. A side consisted of an aluminum frame which held a piece of plate glass 12" x 1-1/6". Between the frame and the aluminum heating plates there was placed a 1/2-inch wide strip of 1/16" Buna-S rubber, a 1/2" deep x 1/2" wide transite insulation strip, and a 1/2" wide layer of glass cloth impregnated with Permatex No. 2. These materials extended at least the vertical length of the heating plates. A cross section of this is seen in the top view of Figure 2. Note that a beam of light passing parallel and adjacent to either heating plate would not touch these materials since they were recessed slightly.

Calming sections were attached to both top and bottom of the heated duct. Cross sections of both were 9.75" wide x 1.04" deep. The top calming section was 24-1/2" in length, the bottom, 8-1/2". Connection was made by means of a thin extension of the heating plates to meet a similar extension in the calming duct sides. These extensions were overlapping, but were separated by means of a 1/4" slab of transite insulation. Connection was made through the 1/4" transite slab by means of 8 stud bolts per side. A short adjustable side was put in the connection between the end of the window

frame and the top calming section. A 1/4" foam rubber gasket plus the movable nature of this piece made possible a correction for differences in thermal expansion. Design of the entire duct was such that the inside dimensions were the same at any point down the duct, with the exception that the distance between the heating plates was 1.01" while the distance between the corresponding faces of the calming sections was 1.04" wide.

Wall temperatures in the heating plates were measured by means of L & N No. 30 B&S glass insulated iron-constantan Duplex thermocouples. These couples were located in horizontal holes which were drilled parallel to and 1/4" from the heat transfer interface. This gave the junction and wire leading to it a 4" isothermal zone in the plate. These thermocouples were located at a distance, x, from the top of the heated plate of 1, 3, 5, 7, 9, and 11 inches.

At the top and bottom of the duct, mechanisms supported a travelling thermocouple which could move anywhere in a plane perpendicular to the heated surface and passing through the axis of the duct. The mechanism of movement could determine horizontal changes in position of the junction within 0.0005" and vertical changes within 1/16". Figure 2 shows the construction.

The travelling thermocouple itself was made by butt silver soldering L&N No. 40 B&S (.0031") copper-constantan bare thermocouple wire. The couple was gold plated for 1" on the copper side of the junction and 3/8" on the constantan side of the junction. This plating and subsequent polishing were done in order to minimize radiation error.

All thermocouple wires led into insulated switch boxes. Separate boxes were used for the copper-constantan and iron-constantan connections. Leads to the potentiometer were

combined through a small switch in one of the boxes. The resulting connection led to a No. 2732 Rubicon Potentiometer. Cold junctions for both the copper-constantan and iron-constantan couples were maintained in the same ice bath in a kerosene filled 1/2" glass tube immersed 8" in a thermos jug of ice-water.

Air was supplied by means of a GE Model No. 150 centrifugal blower. Air passed horizontally from the blower to a sharp right angle bend and then up three feet of 2" brass pipe to a section where a sharp edged orifice was installed. Pipe taps one diameter up and down stream served as both pressure taps for the orifice meter and inlets for thermocouples. A manometer, using air over water, was used to measure the pressure differential across the orifice plate. After another foot of brass tube, the air passed through a 3/4" hose to the top of the flow distributor. The flow distributor served as a housing for the top thermocouple mechanism and as an energy converter for the incoming gas. The air then flowed down through the top calming section and through the heated section of the duct. A narrow slot was formed 1/4" below the heated plates by means of strips of light sheet metal extending inward from each wall. The width of the slot was 0.41" except for a small slit at the center to permit the travelling thermocouple to reach the wall. This construction can be noted by reference to the top and side sectional view of Figure 2.

Tubes were soldered to the outer wall of both the top calming section and the window frames. A controlled flow of water through these tubes maintained the sections at room temperature.

Onto the two outside surfaces of the heating plates were attached 8" x 12" plates of 1/2" thick aluminum. Six equally

spaced 350-watt GE strip heaters were mounted horizontally
on each plate spacing. It was therefore necessary for heat
produced in the strip heaters to pass through one full inch
of aluminum plate in order to gain the inside air-interface
surface; thus uniform distribution of heat was assured.
These strip heaters were connected in parallel in banks of
three, two banks to a side. Power was supplied to these banks
individually as shown in the wiring diagram presented in
Figure 3. This consisted essentially of a variable voltage
transformer between the line and each bank. An additional
circuit was added to enable a wattmeter to be thrown in
between the transformer and the heater.

The optical apparatus set-up is best described by
reference to Figure 4. Light produced by a DC arc lamp was
focused on a stop by means of a Taylor-Hobson $6\frac{1}{2}$" f/2.5 lens.
The stop contained an 0.015" diameter pinhole, which permitted
passage of some of this light. The smallness of the hole
permits consideration of the light as coming from a point
source. The light then passed to an 8" parabolic mirror which
was located at its focal distance (50") from the pinhole. The
reflected light from the parabolic mirror was substantially
parallel and horizontal. A small angle (3.2°) between the
incident and the reflected light means a negligible distortion.
Due to the small refraction of the light rays passing through
the test unit it was necessary to have a long optical path
beyond the unit. Since the room in which the experiments were
conducted was not as long as desired, it was necessary to use
two plane, front-surface mirrors to extend the optical path.
At the point at which the focus of the refracted rays was
desired, an 8" x 10" photographic plate was installed. A $3\frac{1}{2}'$
long wooden rectangular duct extended from the plate toward
the light source to protect the photographic plate from stray
light.

A shutter was installed just beyond the pinhole, to permit a known exposure time on the negative. Film used was Kodak Contrast Process Ortho.

The parallel beam optical path to the test unit was an 8" diameter circle. However, the test section of the test unit was 12" high. Since the optical system once aligned, was very difficult to adjust for accurate work, it was made as a stationary installation. Then, in order to use optical methods on the entire test unit, it was necessary to arrange for vertical movement of the test unit. The unit was, therefore, suspended on a frame in which it could be moved up or down. The weight of the unit was counterbalanced by 128 lbs. of iron sash weights.

A triangular arrangement of three jacks at the base of the supporting framework permitted adjustment of the test rig to vertical. A plumb bob, suspended from an arm, high on the outside of the duct, was used to determine vertical alignment. Near the bottom, the wire supporting the bob passed through a ring. The duct was considered to be vertical when the wire supporting the bob was centered in the ring.

PROCEDURE

The test unit was initially put into operation by supplying power to the blower and heating elements, and cooling water to the cooling tubes for the window frames and top calming section.

About two hours were required for the unit to come to equilibrium which was determined by temperature equality of opposite heating plates, constant wall temperatures, constant inlet air temperature (inlet air was heated by the blower), stability of pressure drop across the sharp edge orifice in the air supply line, and approximate room temperature for the water cooled sections.

After attainment of equilibrium, the test unit was aligned vertically and optically. Vertical alignment was accomplished by changing the length of three jacks supporting the frame so that the plumb bob wire was centered in the ring. The test unit was finally readied by aligning both the parallel incident light and the traveling thermocouple in planes parallel to the heating surfaces.

Traveling thermocouple data were first taken. The junction and wire were first located parallel to the surface at either $y = 0.005"$ or $y = 0.0075"$ from the surface. The junction was then moved vertically down and readings were taken at various values of x inches from the top. A new plane further from the surface was next chosen, and the procedure repeated and so on. The last plane chosen was at $y = 0.500"$ which was close enough to the center to be called the centerline. Actual centerline was at $y = 0.505"$. Only data from one wall to the centerline were collected. Temperature distribution in the gas on the other side of the centerline was assumed to be symmetrical.

All wall temperatures of the heating plate were taken

on the side which was used as the datum plane for the
traveling thermocouple. As a check on the opposite side,
one wall temperature was taken there for comparison.

Pressure readings were taken across the orifice and
between atmosphere and the downstream orifice top. Thermo-
couples installed at the pipe taps gave temperatures at
these points. Finally barometric pressure was recorded.

With lights out, the arc lamp was turned on and
pictures were taken of refraction occuring in the lower
half of the test section. The test unit was then lowered
and similar pictures were taken of the upper half of the
test section. Usually two pictures, of 1/5 and 1/2 second
exposure time, were taken of each section. Standard
procedure was used in development of the negatives.

DISCUSSION

Outline of the Problem. Interest is centered on heat transfer to a fluid forced to flow through a conduit in which gravitational or centrifugal forces are in the direction of the flow.

The temperature gradient from the heated surface to the main body of the fluid produces a change in density in the direction normal to the flow of fluid. The gravitational or centrifugal forces acting on this change in density, produce a difference in hydrostatic head across the conduit. The less dense material near the heated surface, therefore, has less hydrostatic head than the fluid near the center of the duct. Since the fluid pressure normal to the flow is essentially constant across any cross section, this difference in head causes an unbalance of forces, and depending upon the relative strength of these forces, results in reduction, stagnation, or reversal of the downward flow of fluid near the wall.

Since it was not practical to have a simple test unit in which the accelerative force was produced by centrifugal force, the unit had to be so arranged that gravity acted as the effective total of all constant accelerative forces. In the problem under discussion, this was arranged by having a vertical duct as the test unit.

Exact Theoretical Equations. The theoretical equation for heat flow to a moving fluid (1) can be expressed as follows:

$$\frac{\partial t}{\partial \theta} + u_x \frac{\partial t}{\partial x'} + u_y \frac{\partial t}{\partial y'} + u_z \frac{\partial t}{\partial z'} = \alpha\left(\frac{\partial^2 t}{\partial x^2} + \frac{\partial^2 t}{\partial y'^2} + \frac{\partial^2 t}{\partial z'^2}\right) + \frac{q'}{\rho \sigma} \quad (1)$$

The velocity terms in Equation 1 can be expressed by Newton's law, Force = Mass x Acceleration. Newton's equation, applied to motion of unit volume of the fluid in the direction of three coordinates, respectively, (2) becomes:

$$\rho \frac{du_x}{d\theta} = (g_x + P_x + F_x)\, \mathcal{E}_c \qquad (2)$$

$$\rho \frac{du_y}{d\theta} = (\mathcal{E}_y + P_y + F_y)\, \mathcal{E}_c \qquad (3)$$

$$\rho \frac{du_z}{d\theta} = (\mathcal{E}_z + P_z + F_z)\, \mathcal{E}_c \qquad (4)$$

where the total force is composed of:

1. Inertia forces $\mathcal{E}_x$, $\mathcal{E}_y$, $\mathcal{E}_z$, as gravity, or centrifugal force.
2. Dynamical forces P_x, P_y, P_z, as the pressure drop.
3. Frictional forces F_x, F_y, F_z, caused by viscosity and wall friction.

Frictional forces (F) are expressed in the equations of Stokes (3):

$$F_x = \mu\left(\frac{\partial^2 u_x}{\partial x^2} + \frac{\partial^2 u_y}{\partial y^2} + \frac{\partial^2 u_x}{\partial z^2}\right) + \frac{\mu}{3}\frac{\partial}{\partial x}\left(\frac{\partial u_x}{\partial x'} + \frac{\partial u_y}{\partial y'} + \frac{\partial u_z}{\partial z'}\right) \quad (5)$$

Two similar equations (denoted as Eq. 6 and Eq. 7, respectively) for F_y and F_z follow by cyclic variation of x, y, z, and u_x, u_y, u_z.

Exact solution would require simultaneous solution of Equations 1 to 4. However, it is obvious that analytical solution of Equations 1 to 4 is impossible. For practical

purposes, considerable simplification of these equations can be attained without great loss of accuracy. Such simplifications, however, must include laminar flow.

Approximate Theoretical Equations. For the heat conduction equation, Equation 1, such simplifications include the assumption of :

1. Steady state unidirectional laminar flow.
2. Constant physical properties of the fluid (μ, c, ρ, and k).
3. Negligible conduction in the direction of flow, i.e. in direction x.
4. Temperature independent of time.
5. Constant duct wall temperature

Application of these assumptions give:

$$u_x \frac{\partial t}{\partial x} = a(\frac{\partial^2 t}{\partial y^2} + \frac{\partial t}{\partial x^2})$$
(8)

For the hydrodynamic equations, Equations 2 to 7, such simplifications are:

1. P and F are negligible in the direction y and z.
2. Physical properties of fluid are constant with the exception of the density in relation to g, the acceleration due to gravity.
3. Flow is constant and unidirectional
4. Gravitational or centrifugal force lies in the x direction only.

Application of these assumptions to Equations 2 to 7 give:

$$g_x + P_x + F_x = 0$$
(9)

and

$$F_x = \mu(\frac{\partial^2 u_x}{\partial y^2} + \frac{\partial^2 u_x}{\partial z^2})$$
(10)

Since $P_x = -\frac{\partial p}{\partial x'}$ and $g_x = \frac{g_L}{g_c}\rho$, the hydrodynamic equation becomes:

$$-\frac{\partial p}{\partial x'} = \frac{g_L}{g_c}\rho + \mu \left(\frac{\partial^2 u_x}{\partial y'^2} + \frac{\partial^2 u_x}{\partial z'^2}\right) \tag{11}$$

Changes in density are manifest by a change in velocities due to expansion of the fluid and by a change in the gravitational or centrifugal force on a unit volume. Since the former effect has been held constant and the latter has been regarded as a function of temperature, we find that Equations 8 and 11 offer practically the furthest theoretical simplification of the actual case as stated under "Outline of the Problem". Some additional simplification results for the case of flow through a cylindrical tube or between flat parallel plates of infinite extent. But, nevertheless, simultaneous analytical solution of Equations 8 and 11 does not appear possible.

For analytical solution of Equations 8 and 11, it is necessary to regard the density as constant also.

In this case then $\frac{\partial p}{\partial x'} - \frac{g_L}{g_c}\rho =$ Frictional Pressure Drop. So Equation 11 can be expressed as:

$$\left(\frac{\partial p}{\partial x'}\right)_{\text{Friction}} = \mu \left(\frac{\partial^2 u_x}{\partial y'^2} + \frac{\partial^2 u_x}{\partial z'^2}\right) \tag{12}$$

Solution of Equation 12 for flow in cylindrical tubes or between flat parallel plates of infinite extent results in a parabolic velocity distribution (4). Substitution of the parabolic velocity distribution in the heat conduction equation, Equation 8, results in equations amerable to solution.

Norris and Streid (5) have compiled and plotted
these solutions for the cases of parallel infinite plates
and circular tubes. A plot of these equations is given
in Figure 12. Coordinates are listed in Table 12. The
heat-transfer coefficients used are defined by Equation 13.

$$\frac{q}{A} = h_a \left[t_w - \frac{t_2+t_1}{2} \right] = h_i \left[t_w - t_1 \right]$$

$$= h_L \frac{(t_w-t_1) - (t_w-t_2)}{\ln \left[(t_w-t_1)/(t_w-t_2) \right]}$$

$$= \frac{1}{L} \int_0^L h_x (t_w - t_2) \, dx \tag{13}$$

Previous Experimental Work. Stender (6) investigated
the heating of upward or downward flowing water in a vertical
pipe. Flow rates were between a Reynold's Number of 10,000
and 68,000. Little difference was found between heat trans-
fer rates with flow in either direction. He concluded,
therefore, that the buoyant force had negligible effect
beyond $N_{Re} = 10,000$.

Jurgensen and Montillon (7) heated water flowing
within a vertical tube and found the heat tranfer coeffi-
cient independent of flow direction for N_{Re} greater than
20,000. Between the lower limit of investigation ($N_{Re} = 8,000$
to $N_{Re} = 20,000$) they noted that downward flow gave higher
coefficients than either upward flow or flow within a hori-
zontal pipe. Within this range their data for heating water
in downward flow in a vertical tube are correlated by:

$$N_{Nu} = 0.41 \, N_{Re}^{0.54} \cdot N_{Pr}^{0.40} \tag{14}$$

They also mention that Soennecken, (8), who built and first used the apparatus used by Stender, reported higher coefficients with downward than with upward flow.

Colburn and Hougen (9) found that, for heating water flowing in a vertical pipe at rates up to N_{Re} of 2200, the data for that particular tube are correlated by:

$$h = .42 \, t \, (\Delta t_a)^{1/3} \quad \text{for upward flow} \qquad (15)$$

$$h = .49 \, t \, (\Delta t_a)^{1/3} \quad \text{for downward flow} \qquad (16)$$

Experimental Approach to the Problem. Preliminary consideration indicated that if flow rates were low, the fluid could become buoyant enough in the vicinity of the wall to rise against the direction of flow. Under such considerations it was noted that the heat-transfer coefficient may be a function of length and Grashof Number (10) as well as the variables expressed in equations of former work (N_{Re}, N_{Nu}, N_{Pr}). Therefore, it was felt highly desirable to determine local heat transfer coefficients.

One method of determining local coefficients is to obtain the temperature gradient at the wall. Since at the wall the velocity is zero, the heat transfer is by conduction and can be expressed as

$$\frac{q}{A} = 12 k_w \left(\frac{\partial t}{\partial y}\right)_{y=0} \qquad (17)$$

when the gradient is expressed in degrees F. per inch.

If the flow rate of the fluid is not too great, then a linear velocity gradient exists for some distance from the wall. McAdams (11) presents data for air in isothermal

flow, in which the linear velocity gradient extends 0.10 inch from the surface for an average velocity of 7 ft. per second. This distance increases as the velocity decreases.

Martinelli and Boelter (12) give Leveque's solution to the heat conduction equation (Equation 8) for the case of heat transfer to a fluid which has a linear velocity gradient from the heat transfer surface. Their plot of this solution shows that the temperature gradient, too, is essentially linear from the wall.

It is apparent, then, that the temperature gradient at $y = 0$ extends out into the fluid for some distance in cases of low flow rates. Since the velocities at which the buoyant force causes an effect on heat transfer are in the low Reynold's Numbers anyway, this approach should be valid for this investigation.

At least two methods are available for finding the temperature gradients at the wall. One method is to take thermocouple readings at known distances from the wall to find the slope directly. The other is by means of the amount of refraction of light which was initially parallel to the heated surface. Both methods were used and found successful.

Besides these methods, the mixing-cup temperature of air into and out of the heated section was taken as further check. Separate descriptions of each method follow.

Heat Transfer from Traveling Thermocouple Measurements

The hot junction of the traveling thermocouple is adjacent to air at one temperature and essentially surrounded by a heated duct at another. These temperature differences can become appreciable, and the heat transferred to the wire by radiation will cause the wire to be at a higher temperature than the surrounding gas. Since the wire measures its own temperature, this error is introduced in gas temperature measurement.

The radiation error can be calculated by setting up a heat balance around the wire. Heat to the wire by radiation will be equal to heat leaving by convection if the wire is in an isothermal plane. Since the couple is inclosed by a virtual black body, we have:

$$q_{radiation} = q_{convection}$$

$$0.173 \; C L a'' \left(\left(\frac{T_W}{100} \right)^4 - \left(\frac{T_{wire}}{100} \right)^4 \right) = h_x C L (t_{wire} - t_{gas}) \tag{18}$$

Original calculations were made for:

$$T_W = 1060 \; °R \; (600°F)$$

$$T_{wire} = 660 \; °R \; (200°F)$$

$$a'' = 0.84 \text{ for oxidized constantan}$$

$$h_x = 60 \text{ (see Ref. 13)}$$

and resulted in

$$t_{wire} - t_{gas} = 26 \; °F$$

To reduce this error, gold was plated on the junction and polished.

$$\text{Then,} \quad a'' = 0.035$$
$$\text{and} \quad t_{wire} - t_{gas} = 1.1 \, °F$$

However, the introduction of gold onto the surface of the copper to constantan junction causes an additional electromotive force effect. Essentially, a new junction is established between the gold and constantan. The copper to gold plate contact seems to have negligible effect.

Application of a heated rod of known temperature over the point at which the gold plate stopped on the constantan side of the junction indicated that a calculated (14) temperature gradient of 50 degrees F. per inch gave an emf error of about 10 degrees F.

It was then necessary to obtain the length of the gold plate on the constantan side of the junction which would cut down the radiation error at the true junction, and yet be short enough that both major and minor junction had essentially the same environment temperature.

In order to calculate the length of plate needed for this condition, the point at which gold plate stopped on the constantan side of the true junction was considered to be attached to a solid wall of temperature 26 degrees F. (unplated wire to gas Δt). The wire then extended out into an environment of temperature 1.1 degrees F. (minimum protected wire Δt). The solution for this case (14) gives the temperature at any point along the wire.

The final solution of the problem then rests as a balance between the length of plating which will reduce

the error of radiation from 26 °F to "t", versus the
distance between the junction and psuedo-junction which
will raise the error from 0 °F to "t". This length
proved to be 3/8" on the constantan side the junction,
which results in an estimated error of about 3 °F.

On the copper side of the junction there appeared to
be no error introduced by the gold plate; and so the plating
was extended far enough to reduce the error theoretically
to 1.2 degrees F. This length was 1" on the copper side of
the junction. Total length of gold plate was therefore 1 3/8".

The copper constantan wire used for the traveling
thermocouple was Leeds and Northrup No. 40 B&G Gauge (0.0031").
The small size minimized error due to conduction when the
wire lay in a non-isothermal plane. To obtain a point
junction and yet have both joined wires on the same axis,
the junction was made by butt silver-soldering. This was
accomplished by dipping 1/8" of the end of each wire to be
joined into a molten drop of low melting point silver solder.
These two ends were then accurately butted by means of a
micropositioner. A small flame (1/8") was touched to the
junction and the silver-solder flowed into the slight gap
to form a continuous wire. Flux was used in all soldering
operations. So successful was this method that in some of
the couples made, it was not possible to tell exactly where
the junction lay without a low power microscope since color
was obscured for 1/8" on either side of the junction due to
the silver coat.

Gold plate was applied by using a 1-volt potential for
about 20 minutes. The area which rested in the plating
solution but which was not to be plated (only the distance
of 1 3/8" was to be plated) was protected by a coat of

Wonder-Lac stop-off lacquer.

Two different traveling thermocouples were used in the course of all runs. One had a small bead (estimated thickness of 0.004") which identified the junction. The position of the junction of the other could be identified only because its distance from the end of the gold plate on the constantan side of the junction was known.

Slight differences in temperature between the two heated plates or between opposite sides of the top calming section shifted the calming sections slightly from vertical parallel to the heating surfaces. If the traveling thermocouple was flush with the heating surface at one set of conditions, it was found that it might have been displaced 0.020" in the next. Such variation made it desirable to zero the traveling thermocouple before each run.

To zero the thermocouple was not difficult. If the thermocouple wire was close to the heating surface and light was directed at a small angle to the heating surface, then the shadow of the wire on the surface as well as the wire itself could be seen. It can be shown geometrically that the distance between the images as seen is twice the actual distance from wire to plate. Under these conditions the wire can be located with reference to the surface within several thousandths of an inch.

In operation it was found that the wire, although originally parallel to the surface, would not necessarily be parallel when the junction was moved vertically. Fortunately, however, the junction stayed a fixed distance from the wall.

Actually, the error in measure of the distance
between the wall and the wire was not critical, since
the temperature gradient was taken by moving a fixed
horizontal distance from some reference point near the
wall. It made no difference in calculations whether an
attempt was made to fix a standard reference point.

As indicated in "Procedure", at particular points,
x, down the heated duct four temperatures were taken at
specific intervals away from the heating surface.
Temperature measurements taken by means of the traveling
thermocouple were less accurate the farther from the wall
the junction was located. At 0.005" from the wall the
galvanometer was very steady. The farther away the couple
was placed, the more the galvanometer oscillated. In some
cases, duplication of results could not be secured within
0.2 millivolt for y = 0.10" from the wall.

Despite this error, slopes were easily found by use
of the four points. Cases in which the error was large
due to the eddying of the gas were cases of large
temperature gradients anyway and the percent error was
approximately the same in all.

Temperature measurements for gradients near the start
and end of the heating section (x = 0, 11.75") were the
most in error. At the start of the heating section, the
temperature measurements gave a curve up to the wall. The
gradient at this point was estimated and is listed in the
data (Table VIII), but was so obviously in error that the
gradient as determined by the optical method was
substituted for calculation of the heat flow. Near the
end of the heated plate (x = 11.75"), the disturbance due
to the contraction (located 1/2" farther down) as well as

a drop-off of plate temperature due to conduction to the lower calming section, seemed to cause peculiar results. With these exceptions results were good.

As expressed in Equation 17, the heat transfer rate per unit area is known if the temperature gradient in air at $y = 0$ and the thermal conductivity are known. To find the total heat to the air it is necessary also to define the area of heating surface from which this heat passes.

The length of the heating plates which was 12", is defined as the heated length. The width of the heating plates was 8". At the edges, however, there was a 1/2" transite strip and a 1/16" rubber gasket through which the temperature dropped from t_w to the cooled-windowframe temperature (about room temperature). The heating width was therefore approximately the eight inches of aluminum plate plus one-half of the distance through the transite-gasket insulation on each extreme or 8.56".

It was assumed that the point temperature gradients as found at the center line existed across the heated width. Under this assumption, the average temperature gradient is expressed as:

$$\left(\frac{\partial t}{\partial y}\right)_a = \int_0^L \left(\frac{\partial t}{\partial y}\right)_x \frac{dx'}{L} \tag{19}$$

For this integration, the gradients $\left(\frac{\partial t}{\partial y}\right)_x$ were plotted versus x (but the temperature gradient at $x = 0$ was taken from the optical data). The resulting graph was then integrated by using Gauss's 6 point integration formula (15). Then:

$$q = 12 \, k_w A \left(\frac{\partial t}{\partial y}\right)_a \tag{20}$$

where $(\frac{\partial t}{\partial y})_a$ is expressed in degrees per inch. A in this
case is 2 x 8.56 x 12.00/144. = 1.425 sq. ft.

Values of the temperatures from which temperature
gradients were calculated, temperature gradients, and q_t
calculated from these gradients, are listed in Tables
III, VIII, and X, respectively.

Heat Transfer from Visual Measurements

Jakob (16) points out that if a heated plate in air
has a constant temperature gradient from the surface for
a short distance, then the refraction of a grazing beam
of light over this surface can be used to measure the
temperature gradient. We have already noted, in the flow
range to be studied, that a linear temperature gradient
exists for some distance from the wall into the fluid.
The method then appears ideal for the present study.

Martinelli et al. (17) outline the mathematical
derivation of the equation for calculation of the
temperature gradient from amount of refraction:

$$(\frac{\partial t}{\partial y})_{xV} = \frac{-Y_s T_w^2}{0.144 \, \beta} \quad \frac{760}{P_b} \quad \frac{1/12}{a_h L_{opt}} \tag{21}$$

where β is a correction factor which effectively replaces
T_w by an average temperature through which the light passes
in the course of refraction, and is expressed by the
equation:

$$\beta = 1 + \frac{0.31}{.144} (\frac{Y_s}{L_{opt}})^2 \quad \frac{760}{P_b} \quad T_w \tag{22}$$

The test unit as described under "apparatus" comprised a flat duct with two parallel, opposite heating surfaces as the wider sides, and glass windows as the narrower. With two parallel plates, the obvious method of obtaining grazing light is with parallel light. Figure 4 shows the equipment arrangement to obtain parallel light.

Idealized operation of the test unit for visual purposes is best noted by reference to the lower right hand view on Figure 5. This view presents the test duct as if looking down from above. Air is passing into the plane of the paper. Light which is originally grazing and parallel to the heated surface is refracted from the heated surface. After leaving the duct the light resumes a linear path, but with the deviation it had upon leaving the test unit. A screen is set up beyond the test unit to intercept the refracted light. The distance is measured between the point at which this light falls upon the screen after passing by the heated plate, and the point at which it falls if no heat is applied to the unit (no deviation). Since the distance of the screen from the test unit is known, the temperature gradient through which this grazing light passes can be calculated from Equation (21).

The main graph of Figure 5 shows the amount of refraction of the light in relation to the temperature through which it passes. The solid, arrow marked lines indicate light which has just left the test unit ("Emergence of Light from Test Unit"), after having passed perpendicular to the dotted temperature profile shown under the main diagram.

The refraction of the light beam, such as beam AA,
which just grazes the heated surface is of interest. Its
distance of refraction on the screen is measured from a
linear extension of the heated surface to the indicated
point. Total distance of refraction is Y_g. Note however,
that beam BB which initially was parallel but not adjacent
to the heated surface was refracted even more than beam AA.
This was caused by the fact that beam BB has passed through
the same temperature gradient, but at a lower absolute
temperature than beam AA. Review of Equation 21 will show
that this condition is expected to give a larger refraction.

Beam CC, which is typical of light passing through the
center of the duct, is refracted little because of the low
temperature gradient. These beams form a bright center line
on the screen.

Example of these patterns of refraction can be noted by
reference to Figure 6, Run E-4.

If the screen is brought to within 2 to 5 feet of the
test unit, the convergence of rays BB and CC indicate
closely the point of actual penetration of heat to the gas.
In some cases also it is a measure of a laminar film. In
all cases, the refraction is so slight at this distance,
that the image as seen gives essentially the actual distance
between heated films. Figure 8 shows full size pictures of
such "close-up" for the upper and lower section of the test
unit.

Due to the lack of linear length beyond the test unit,
it was necessary to install two plane front-surface mirrors.
Since the standard front-surface mirrors are not optically
plane, it was necessary to correct for deviations.

After exhaustive tests, it was found that horizontal deviations were negligible. Vertical deviations, however, resulted in a 1/4" contraction of the image. Correction of this problem rested on placement of a "ladder" in front of the test unit window. This ladder had rungs which cut off the entering light at known intervals down the heated length. The resulting photographs then had these markings which located exactly where the light had come from. This procedure also helped correct for vertical refraction.

In some cases, it was desirable to put a stop in the light path to cut out all of the light which would otherwise have passed through the center of the duct, (such beams as CC in Figure 5). Only a vertical slab of light 0.07" thick and adjacent to each heated surface was permitted to pass across the duct. Figure 7 shows photographs taken with and without the stop.

As noted in the section headed "Apparatus", it was necessary to move the test unit up and down since the unit was greater in vertical length than the height of the optical path; the parabolic mirror was only 8" in diameter whereas the length of the test unit used for pictures was from x = 0 to 11.75. Therefore, it was necessary to readjust the position of the unit for each run, and to realign the heating surfaces parallel to the parallel light. However, such alignment was not difficult. If parallel light was passing between the two polished parallel plates in the test unit, and the plates were turned slightly, then some light would strike one of the plates and be reflected. If a screen was set up about 3' from the exit of the light rays from the test unit, a sharp line was found to be superimposed upon the usual

light through the unit. This line approached coincidence
with the boundary of light only when the plates approached
being parallel with this parallel light. If the unit was
twisted past the point of being parallel, then the same
phenomena occurred although propagated from the opposite
plate. In short, alignment at the point at which no
reflected lines appeared on the screen was assurance of
the parallel nature of both light and plates. Addition
of heat, which refracted the light causing slightly non-
parallel beams, caused no apparent effect on this procedure.

As already brought out, the measurement of the
deflection of the refracted beam of light which grazes the
heating surface (Beam AA in Figure 5) is necessary to find
the temperature gradient. As can be seen by reference to
Figure 4 or 5, the grazing beam starts from one side,
crosses the horizontal centerline and appears on the screen.
The distance deviated (Y_g) then is:

$$Y_g = \frac{\text{Distance between inner boundaries on screen} + 12D}{2} \quad (23)$$

where, in this unit, $D = 1.01/12$ feet.

The wall temperature of the heated plate was constant
across the aluminum plate but dropped off linearly through
the transite-gasket strip to the window frame. As discussed
previously, one-half of the thickness of the strip on either
side is considered to be a part of the heating section.
Equation 21, however, contains an absolute wall temperature
term. It therefore becomes necessary to correct for the
fact that over this section a different $(\partial t/\partial y)_x$ and T_w
exist.

Two assumptions are made:

1. That the average temperature (T_w') of the transite-

rubber strip is the arithmetic average between T_w and the
window frame temperature (taken as 100 F), or:

$$T_w' = \frac{T_w + 560\,°R}{2} \qquad (24)$$

2. That the average temperature gradient through
which the light passes in this region is one-half of the
gradient from the aluminum plate.

Suppose that we now say that one unit length of
aluminum plate under temperature T_w and gradient $(\partial t/\partial y)_x$
gives a deviation (Y_s). Under identical circumstances
then, we find what deviation (Y_s') would occur for unit
length of the transite-rubber strip. Solving Equation 21
for Y_s and setting up the ratio of deviations with the
stated assumptions gives

$$Y_s'/Y_s = (\tfrac{\partial t}{\partial y})_x \,(1/T_w'^2) \,/\, 2\,(\tfrac{\partial t}{\partial y})_x\,(1/T_w^2) \qquad (25)$$

In the case of when $t_w = 500\,°F$, the ratio is 0.800.
This means that one unit length of the transite-rubber
insulation strip is equivalent to 0.800 units of the
aluminum plate with respect to refracting the passing
light. The effective heating length based on T_w for this
case is, therefore, the length of the aluminum plate plus
0.800 times the transite length (which is 18/16"). This
gives a value of $a_h = 8.90"$. The accepted value for this
unit (as was explained previously) is 8.56". To avoid
complications, it was decided to multiply Equation 21
directly by the correction factor of the standard a_h to
the new a_h. Such correction factors for $t_w = 500$, 400,
300, 200, and 100 °F are, respectively, 0.958, 0.968,
0.978, 0.987, and 1.000.

The value of $(\partial t/\partial y)_{xv}$ for any particular value of x is then calculated by use of Equation 21, remembering that:

1. Y_s is calculated by Equation 23 from the photographic record.

2. T_w at x is obtained from a graph of Table 5.

3. The aforementioned correction factor is applied.

4. Barometric pressure is allowed for.

Use of these values gives the calculated values of $(\partial t/\partial y)_x$ as tabulated in Table IX.

The total heat transferred to the air from this section is calculated precisely as described for the case of temperature gradients by traveling thermocouples. As before, use is made of Equations 19 and 20.

Values of Y_s, gradients, and q_v from these gradients are listed in Tables VII, IX, and X, respectively.

Heat Transfer as Calculated by Average Inlet and Outlet Temperatures

The standard method of measuring the heat to a fluid is to obtain the heat input and subtract losses. Such a method was impractical in this case due to the unusual design of the apparatus as well as low heat pick-up by the air. In such case it was felt that more accurate information might be obtained by taking the average inlet and outlet temperatures. The method is:

$$q = Wc(t_1-t_2) \qquad (26)$$

The flow rate ranged up to a maximum Reynolds number of 4900. Under these conditions the velocity profile at the start of the heated section was very closely parabolic (18). With the temperature profile also at the start of the heating section, it was possible to find the average temperature (t_1) at $x = 0$, based on the assumption that there was a two dimensional velocity and temperature field.

The average velocity is given by the equation:

$$u_{av} = W / S (\rho_0 T_0 / T_1) \tag{27}$$

and the point velocity is given by

$$u = \frac{6}{D^2} u_{av.} (Dy'-y^2) \tag{28}$$

The point density is related to the main body density by the equation

$$\rho = \rho_0 T_0 / T \tag{29}$$

and the mass flow rate is given by

$$W = a \int_0^D u \rho \, dy' \tag{30}$$

where D is in feet.

Equation 27 is substituted into Equation 28. Equations 28 and 29 are substituted into Equation 30. Solution for the average temperature (T_1) gives

$$1/T_1 = \frac{6}{D^3} \int_0^D (Dy'-y^2) \, dy' / T \tag{31}$$

This equation was solved by ploting T versus y at $x = 0$. Temperatures were then picked off at points which corresponded to values of y which would fit in Gauss's six-point integration formula (15). The entire equation was then numerically solved by use of Gauss's formula. Table I gives the inlet temperature profile. Table X gives T_1.

A similar principle was used to find the mean outlet temperature. At a distance of 1/4" below the end of the heating plate, a contraction was set into the duct. The form of this contraction which is effectively a narrow slit running the full width of the duct, can be noted by observing the top view of Figure 2. It is well known that a constant velocity exists in a stream passing through such contraction (19). Therefore, the same method of calculation used at $x = 0$ can be used at the contraction. Equations for this case are identical with the former except that $u = u_{av.}$. Solution gives:

$$1/T_c = \frac{1}{D'} \int_0^{D'} \frac{dy}{T} \tag{32}$$

where D', expressed in inches, equals the diameter of the contraction (0.410").

It is to be noted, however, that the contraction was 1/4" below the heated section. In order to obtain the heat transferred to the gas in the heated section for comparison with the other two methods of obtaining heat transfer, a correction factor must be applied.

It was assumed that this strip, below the heated section, was 50% effective, or that the amount of heat transferred from $x = 0$ to the contraction was equivalent

to the amount transferred if the heating plate had been
12-1/8" long.   Therefore:

$$q_h = \frac{12.00}{12.12} W_c (t_1 - t_c)$$ (33)

The flow rate was metered by means of sharp edge
orifices which had been calibrated with calibrated gasometer.
Orifice coefficients were as expected. Calibration error
was estimated to be 1%, but, due to slight variations in
the input voltage to the blower, usage error was advanced
to 2%.

The specific heat at constant pressure was taken as
0.240 plus .003 correction for humidity.

The values of q_h calculated from the mean temperature
change are listed in Table X.

Consideration of Data for Analysis

In geometrical configuration, the test unit is a
narrow rectangular duct. Nevertheless, it cannot be
considered to be a true heated duct, since only two of
the sides are heated. In a case such as this, it can be
assumed that the two parallel heated plates are a slice
cut from the classical case of air flowing between two
heated planes of infinite extent.

We will choose the breadth of the section cut from
the infinite plates as equal to the heated breadth (a_h)
of the unit. Formerly, then, the cross sectional area
was 9.75" x 1.01", now an imaginary piece has been taken

out of each end and the new area is 8.56" x 1.01". The
former breadth of 9.75" was not fully heated at the
extremes; the new heated breadth can, as was discussed
previously, be considered to have the full plate
temperature t_w.

It remains then to correct for the fact that the
average velocity in the removed area is much lower than
in the center "core" area.

Semiquantative relationships (20) show that if the
point of cut-off is specified, a relation exists between
the velocity at the cut-off point and the velocity at a
specific distance from the wall in the center of the duct.
In this case, the velocity at the cut-off is approximately
the same as at 0.17 D from the heated surface in the
center of the duct. Since at the center of the duct, the
velocity from the wall is closely parabolic, the average
velocity flowing through the cut-off end section may be
approximated by:

$$u_{av.} = \int_0^{.17D} 6\, u_m \left(\frac{y'}{D} - \frac{y^2}{D^2}\right) dy' = 0.5\, u_m$$

It will be assumed that the weight flow is proportional
to the linear velocity. The "core" area is 88% of the old
area. Therefore the weight rate in the "core" can be
expressed by use of the area and velocity relationships
mentioned. Then,

$$W_h = 0.88\, W + \frac{0.12}{2}\, W \tag{34}$$

$$= 0.94\, W$$

$$G_h = \frac{0.94\, W}{S_h} \tag{35}$$

where $\quad S_h = a_h D = \dfrac{8.56 \times 1.01}{144} = 0.0601 \text{ sq. ft.}$ (36)

Note that the extremes of error for flow down this "core" are $\pm$ 6%. These extremes are: 1) no flow in the excluded cross section, and 2) uniform velocity over the entire cross section of the duct. Probable accuracy of flow down this "core" is $\pm$ 2% of the true flow.

For purposes of consistency, all future calculations concerning heat transfer coefficients will be based on G_h. This assumes that all of the heat goes into the amount of air expressed as G_h. Such is not the case as some mixing occurs. Error introduced in this assumption affects the value of the calculated heat transfer coefficient (h_a) since it is based on the arithmetic average temperature rise between two points. However maximum error from this assumption proves to be 1.8% and decreases quickly as the flow rate increases.

Range of Investigation

Flow rates of runs are identified by letters, thus:

Approximate Reynolds Number,	900	1800	2700	3600	4800
Identifying letter,	A	B	C	D	E

Wall temperatures are identified by numbers, thus:

Approximate Wall Temperature,	200	300	400	500
Identifying number,	1	2	3	4

If two runs were made at the same general conditions, they are differentiated by a letter "a" or "b" after the number.

All combinations of conditions involving the five letters and four numbers were made. One special run (x-4) had a Reynolds number of 1440.

RESULTS

Comparison of the Three Methods

The optical method of determining temperature gradients in the air adjacent to the wall agrees very well with thermocouple measurements. Based on the total heat transfer from the heated section as calculated by temperature gradients, Equation 20, q_t was found to agree with q_v within an absolute error of 3.8% and an average error of 1.1%. Despite the good agreement, optical measurements were found to be more consistent.

The heat to the section as calculated from the air inlet and outlet mean temperatures, Equation 33, gave an absolute difference of 21.5% and an average of +7.0% from q_v. Results obtained from the inlet and outlet air temperatures were not consistent. For instance in runs C-4, D-4, and E-4, optical pictures showed the usual pattern for forced flow with no apparent buoyant effects; nevertheless, as the flow rate increased in these runs q_h decreased. This is contrary to all previous evidence.

Due then to the greater consistency and more likely accuracy, it was decided to use $q_v = q$ for all future calculations.

Mechanism Analysis

Variation in the local heat transfer as the flow rate decreases (E to A) can be noted by reference to Figures 10 and 11. These plot variation in temperature gradients (which are proportional to q/A) versus x for a particular wall temperature (500 °F). The D and E runs follow the

expected variation in that q/A decreases approximately by $(1/x)^{1/3}$ (note Figure 15). As the flow velocity decreased, however, a "hump" appeared in the curve. The exact description of this phenomena can be best illustrated by reference to Run X-4.

A plot of the approximate theoretical variation of the heat transfer coefficient with the actual local coefficient in Run X-4 is given in Figure 14. With the entering Reynolds number at 1440 the flow was essentially laminar. As the gas passed into the heated section, heat flowed from the wall into the gas in accordance with Equation 8. With the low flow rate, the gas near the wall became buoyant and its velocity became slower than isothermal flow calculations would indicate. This stagnation of flow near the wall caused a decrease of the heat transfer below what would be expected.

Before the gas near the wall flowed much farther, its density change was sufficient to cause upward flow at the wall. Such upward flow created a semi-turbulent condition. The heated layers near the wall are thrown into the core of the gas stream. This, therefore, effectively brought the core temperature much nearer to the wall and a sharper temperature drop occurred per unit distance from the wall. As can be seen, a sharp increase in the heat transfer resulted.

The semi-turbulent condition and rapid heat transfer rate raised the core temperature quickly. Since the buoyant effect depended upon the density difference between the core and the gas adjacent to the wall, a decrease in the velocity of the gas near the wall resulted. This stagnation again reduced the heat transfer. At some point then the temperature of the core had become close enough to that of the wall so that the flow shear again reverted the wall film to downward flow. Run A-4, Figure 10 shows the beginning of this condition.

Reference to Figure 9 shows the temperature profiles
at different values of x in Run X-4. At x = 1" and 4" it
is obvious that laminar flow was still controlling the heat
flow. By x = 7", it can be seen that the semi-turbulent
condition caused by upward flow at the walls had greatly
increased the core temperature and the temperature gradient
at the wall. Farther evidence of this phenomena can be
noted by attention to Figure 8.

As discussed previously, Figure 8 shows essentially
the exact boundary of the heated film. Note that the
upward flowing film seems to tear off into the main core.
This variation of the film thickness causes fluctuations
in the local heat transfer coefficient with time. Note the
waviness of the outer boundary of light. This light had
passed adjacent to the heated surface. Indentations
indicate where the temperature gradient was momentarily
steeper. Variations in gradient with time made it necessary
to average a number of photographs; however, variation
between views was not excessive as can be noted by observing
Figure 7.

It is of interest to note that even under these
turbulent conditions the gradient was approximately a
straight line to y = .1". Maximum deviation (Run E-4) of
initially grazing light was 0.05" from the heated surface
when leaving the unit.

If the Runs A-1, A-2, A-3, and A-4 are examined they
are found to increase in temperature and to have approximately
equal Reynolds numbers. The buoyant counterflow is seen to
become more apparent as the temperature increases. Increase
in temperature or decrease in flow rate thus are, as expected,
variables which increase the tendency for the upward flow.

Comparison and Analysis

Norris and Streid[5] have collected and plotted
some of the complex analytical solutions for heat transfer
to a fluid flowing in steady state laminar flow. These
equations assume constant physical properties and constant
wall temperature. A plot of these equations is given in
Figure 12. Coordinates are tabulated in Table XII. Heat
transfer coefficients as expressed in these equations are
defined by Equation 13.

Using q_v over the 12 inch long heated section (Table X)
we found the temperature rise of the air flow G_h from t_1 to
t_2. Combining D_e, Equation 13, and 20, we obtained the
average Nusselt number (notice that for infinite plates
$D_e = 2b$).

The data are plotted against the coordinates of
Figure 12. The line for the average Nusselt number for
flat ducts (infinite plates) from Figure 12 is also plotted
on the same graph. These results are presented in Figure 13.

Since k_w does not vary much with air, the decrease of
the function ϕ is largely due to the drop of G_h in value.
It is noticed then that as G_h decreases, the data fall under
the theoretical curve. This could be caused by two effects:

1. The resulting slowing down of the film due to the
increased buoyant effect on the slower fluid.
2. Emergence from the lower transition into the fully
laminar region of flow. No matter which effect predominates,
the data are no less than 25% under the theoretical equation.

As soon as the flow rate becomes low enough to cause a
reversal of flow near the wall, the Nusselt number climbs
again to values over the theoretical. However, when the
buoyant forces are of the same order of magnitude as the
forced flow forces (as the data are), the upward flow will
again approach the theoretical.

Therfore in the range investigated, it can be said that the average Nusselt number will be within ±25% of the values predicted by the plots of Figure 12.

In the case of small L/D ratios as say 1.5 in Run X-4, (Fig. 14) such statements may not be true; however such a small L/D would rarely be found.

In the range in which the buoyant force is much greater than the forced flow forces, it appears that the Nusselt number would approach values given by heat transfer to a cooler fluid in a vertical tube, the lower end of which is closed.

BIBLIOGRAPHY

1. Jakob, M., Heat Transfer, Vol. I, Wiley and Sons, N.Y. 21-22 (1949)

2. Jakob, M., Heat Transfer, Vol. I, Wiley and Sons, N.Y. 17-18 (1949)

3. Stokes, G. C., Trans. Cambridge Phil. Soc. $\underline{8}$, 287 (1845)

4. Rouse, H., Elementary Mechanics of Fluids, Wiley and Sons, N.Y. 154-157 (1946)

5. Norris, R. H., and Streid, D. D., Trans A.S.M.E., $\underline{62}$, 525-533 (1940)

6. Stender, Wiss. Veroffentlich. Siemens - Konzern, $\underline{9}$, 88 (1930)

7. Jurgensen, D. F., Jr., and Montillon, G. H., Ind. Eng. Chem. $\underline{27}$, 1466 (1935)

8. Soennechen, Forsh. Arb. Heft 108/109, 33 (1911)

9. Colburn, A. P., and Hougen, O. A., Ind. Eng. Chem. $\underline{22}$, 522 (1930)

10. McAdams, W. H., Heat Transmission, 2nd Edition, McGraw-Hill, N.Y. 191 (1942)

11. McAdams, W. H., Heat Transmission, 2nd Edition, McGraw-Hill, N.Y. 104 (1942)

12. Martinelle, R. C., and Boelter, L.M.K., Univ. of Calif. Pub. in Eng., Univ. of Calif. Press, Los Angeles. $\underline{5}$, 23-58 (1942)

13. Mueller, Trans. Amer. Inst. Chem. Eng. $\underline{38}$, 613 (1942)

14. Boelter, L. M. K., Cherry, V. H., Johnson, H. A., Martinelle, R. C., Heat Transfer Notes, Univ. of Calif. Press, Los Angeles. IIb-9 (1948)

15. Milne, W. E., Numerical Calculus, Princeton Univ. Press, Princeton, N. J. 285 (1949)

16. Jakob, M., Heat Transfer, Vol. I., Wiley and Sons, N.Y.
     568 - 577 (1949)

17. Boelter, L. M. K., Cherry, V. H., Johnson, H. A.,
     Martinelle, R. C., Heat Transfer Notes, Univ. of Calif.
     Press, Los Angeles. XII 21 - 28 (1948)

18. Goldstein, S., Modern Development in Fluid Dynamics, Vol.
     I, The Clarendon Press, Oxford. 310 (1938)

19. Powell, Mechanics of Liquids, MacMillen, N. Y. 123 (1940)

20. Rouse, H., Elementary Mechanics of Fluids, Wiley and Sons,
     N.Y. 215 (1946)

NOMENCLATURE

A   = surface area of that part of duct which transfers heat (for a flat duct it includes both sides if both are transferring heat), sq ft

a   = longest side in the perimeter of a duct, ft

a_h = heated portion of a

b   = shortest side in the perimeter of a duct, ft

C   = 2a+2b = perimeter, ft

C_o = orifice discharge coefficient, dimensionless

c   = specific heat (at constant pressure), BTU/lb/°F

D   = diameter or distance between plates for a flat duct, ft

D_o = D for orifice flow meter

D_p = D for the pipe at the flow meter

D_e = equivelent diameter = 4S/C, ft

F   = frictional force, lb force/sq ft/ft

G   = W/S = weight velocity, lb/sq ft/hr

G_h = G based on S_h, lb/sq ft/hr

g_c = conversion factor, lb mass ft/lb force hr^2

g_L = acceleration due to gravity or centrifugal force ft/hr^2

h   = heat transfer coefficient based on particular temperature differences indicated by subscript used with h, as defined by Equation 13, BTU/hr/sq ft/°F

h_a = h on arithmetic-mean-temperature basis (see Equation 13)

h_i = h on inlet-temperature-difference basis (see Equation 13)

h_L = h on logarithmic-mean-temperature basis (see Equation 13)

h_x = h on local-temperature-difference basis (see Equation 13)

k_w = thermal conductivity of fluid at wall temperature, BTU/ (hr) (sq ft) (^{o}F)/(ft)

L = distance from entrance of heated portion of duct, ft (unless otherwise stated)

L' = portion of traveling thermocouple wire exposed to radiation, ft

L_{opt} = optical length measured from center of heating plate to screen, inches

N_{Pr} = $c\mu/k$ = Prandtl number, dimensionless

N_{Re} = GD/μ = Reynolds number, dimensionless

N_{Re_o} = N_{Re} through the orifice

N_{Re_1} = N_{Re} based on inlet temperature (t_1)

N_{Nu_a} = $h_a D/k$, average Nusselt number, dimensionless

P = pressure drop, lb force/sq ft/ft

p = absolute pressure, lb force/sq ft, unless otherwise stated

P_b = barometric pressure, cm water

P_b' = barometric pressure, mm Hg

P_d = absolute pressure at the downstream flow meter pipe tap, cm water

P_u = absolute pressure at the upstream flow meter pipe tap, cm water

q = total heat transfer, based on a particular method of arriving at the result as indicated by the subscript used with q, BTU/hr

q_h = q based on temperature rise of the air through the test unit (see Equation 33)

q_t = q based on $(\partial t/\partial y)_{aT}$ as calculated from thermocouple readings at fixed distances from the wall (see Equation 20)

q_V = q based on $(\partial t/\partial y)_{aV}$ as calculated from visual measurements (see Equation 20)

q' = heat energy developed in unit volume and time, BTU/hr/cu ft

S = cross sectional area for fluid flow, sq ft

S_h = S for the area $a_h b$, sq ft

T = absolute temperature designation of t, deg R

t = fluid temperature, deg F

t_m = traverse mean (mixing cup) temperature of the fluid, deg F

t_1 = t_m at entrance of heated portion of duct, (x=0), (see Equation 31)

t_2 = t_m at any distance (x) down heated portion of duct

t_c = t_m at contraction (see Equation 32)

t_o = reference fluid temperature, or average temperature at the flow meter, deg F

t_w = wall temperature, deg F

t_a = $t_w - (t_1+t_2)/2$, deg F

u = velocity, ft/hr

u_m = u average for the entire cross section of duct

u_x = u in x direction

u_y = u in y direction

u_z = u in z direction

W = total mass flow rate of fluid, lb/hr

W_h = W through the "core" cross section ($a_h b$) (see Equation 34)

x = axial distance from the entrance of heated portion of duct, inches

x' = x in dimensions of feet

Y_s = measured screen deviation of refracted light, inches (see Figure 5)

y = shortest distance between the heated surface and the duct axis and is measured from the wall, inches

y' = y in dimensions of feet

z = distance perpendicular to the duct axis and parallel to the heated surface, inches

z' = z in dimensions of feet

α = $k/\rho c$, thermal diffusivity, sq ft/hr

α'' = absorbtivity, dimensionless

θ = time, hr

μ = viscosity of fluid, (lb force)(hr)/(sq ft)

ρ = density, lb/cu ft

ρ_o = ρ at temperature t_o, lb/cu ft

$\left(\dfrac{\partial t}{\partial y}\right)$ = air temperature gradient at the heated surface (y=0), deg F/ inch

$\left(\dfrac{\partial t}{\partial y}\right)_x$ = $\dfrac{\partial t}{\partial y}$ at x

$\left(\dfrac{\partial t}{\partial y}\right)_{xT}$ = $\left(\dfrac{\partial t}{\partial y}\right)_x$ as determined from traveling thermocouple measurements

$\left(\dfrac{\partial t}{\partial y}\right)_{xV}$ = $\left(\dfrac{\partial t}{\partial y}\right)_x$ as determined from optical measurements

$\left(\dfrac{\partial t}{\partial y}\right)_a$ = $\displaystyle\int_0^L \left(\dfrac{\partial t}{\partial y}\right)_x \dfrac{dx'}{L}$, deg F/inch

$\left(\dfrac{\partial t}{\partial y}\right)_{aT}$ = $\left(\dfrac{\partial t}{\partial y}\right)_a$ as determined from traveling thermocouple measurements

$\left(\dfrac{\partial t}{\partial y}\right)_{aV}$ = $\left(\dfrac{\partial t}{\partial y}\right)_a$ as determined from optical data

ϕ = $\dfrac{c \omega D^2}{kL}$, dimensionless

APPENDIX A - SAMPLE CALCULATIONS

1. Calculation of Y_s.

Using $x = 3''$ from Run E-4 as an example, we find from the primary data that:

$$A = 1.425 \text{ sq ft}$$
$$a_h = 8.56/12 \text{ ft}$$
$$D_e = 2b = 2D = 2.02/12 \text{ ft}$$
$$k_{w_{ave}} = 0.0243 \text{ BTU/(hr)(sq ft)(deg F)/ft}$$
$$L_{opt} = 563 \text{ inches}$$
$$P_b' = 1040 \text{ cm water} \times 1.357 = 766 \text{ mm Hg}$$
$$T_{w_{x=3''}} = 495.0 \text{ deg F} = 955 \text{ deg R}$$
$$t_{w_{ave}} = 494.9 \text{ deg F}$$
$$Y_s = 2.240 \text{ inches}$$

from Equation 22 then:

$$\beta = 1 + \frac{0.31}{0.144} \left(\frac{2.240}{563}\right)^2 \frac{(760)(955)}{766} = 1.0322$$

Substituting in Equation 21 and multiplying by the correction factor as indicated on page 29 gives:

$$\left(\frac{\partial t}{\partial y}\right)_{xV} = (0.958) \frac{(2.240)(955)^2(760)(1/12)}{(0.144)(1.0322)(766)(8.56/12)(563)}$$
$$= 2720 \text{ deg F/inch}$$

2. Calculation of q_V.

Calculation of the average value of $\left(\partial t/\partial y\right)_{xV}$ over the length L can be accomplished by graphical use of Equation 19. $\left(\partial t/\partial y\right)_{xV}$ is plotted versus x and either graphically integrated or specific points are taken which fit Gauss's numerical integration formula (15). Such an

integration for Run E-4 gives:

$$\left(\frac{\partial t}{\partial y}\right)_{aV} = 2552 \text{ deg F/inch}$$

The heat flux to the air through the test unit is expressed in Equation 20 as:

$$q_V = 12 k_w \left(\frac{\partial t}{\partial y}\right)_{aV}$$

Substituting the above values gives:

$$q_V = (12)(0.0248)(1.425)(2552) = 1042 \text{ BTU/hr}$$

3. Calculation of N_{Nu_a}

A graphical plot of the temperature profile at the start of the heated portion of the duct ($x=0$) in conjunction with Equation 31 gives t_1. This is accomplished either by graphical integration or use of Gauss's numerical integration. For Run E-4, $t_1 = 107.1$ deg F.

Solving for t_2 in Equation 26 gives:

$$t_2 = t_1 + \frac{q_V}{\overline{w_h} \overline{C}}$$

$$t_2 = 107.1 + \frac{1042}{(0.0237)(0.94)(3600)(0.243)} = 160.5$$

then,

$$\Delta t_a = 494.9 - \frac{160.5 + 107.1}{2} = 361.1 \text{ deg F}$$

Combining Equations 13 and 20 and multiplying both sides by D_e, we have:

$$N_{Nu_a} = \frac{h_a D_e}{k_w} = \frac{12 \left(\frac{\partial t}{\partial y}\right)_{aV} D_e}{\Delta t_a} = \frac{(12)(2552)(2.02/12)}{361.1}$$

$$= 13.72$$

TABLE II

CONTRACTION TEMPERATURE[#] PROFILE
AT DISTANCE, x, = 12 1/4" FROM THE TOP

RUN NO.	Distance from Wall, y, Inches				
	.300	.350	.400	.450	.500
A-1	152.0	146.8	142.0	137.5	137.6
A-2	207.2	200.4	189.5	182.5	181.1
A-3	280.5	269.0	263.7	249.3	248.0
A-4	355.9	339.2	329.6	319.4	311.1
X-4	295.1	280.7	259.9	240.1	235.3
B-1a	139.3	130.6	114.7	107.9	105.6
B-1b	146.4	137.0	123.1	112.5	111.6
B-2a	170.2	158.5	148.4	133.1	127.7
B-2b	194.8	174.6	154.1	137.3	131.0
B-3	205.4	189.7	180.8	172.5	168.5
B-4	256.7	241.6	229.0	218.7	212.6
C-1a	132.3	120.6	109.7	101.0	101.5
C-1b	143.0	126.6	118.2	111.5	112.4
C-2a	159.7	140.9	121.0	108.5	107.9
C-2b	170.0	153.3	132.3	119.9	119.8
C-3a	206.4	180.9	155.3	137.3	129.5
C-3b	204.2	179.4	155.3	136.3	131.0
C-4	252.4	207.2	181.2	162.6	149.8
D-1a	126.0	113.6	103.6	101.4	102.6
D-1b	136.0	124.1	116.5	112.9	113.1
D-2	162.2	138.9	119.7	110.6	110.7
D-3	196.7	174.8	135.2	123.4	121.2
D-4	243.9	194.8	159.3	141.8	142.4
E-1	132.7	121.4	114.6	112.4	112.6
E-2	157.7	132.4	123.9	117.5	118.8
E-3	176.8	145.5	126.8	118.8	121.1
E-4	212.4	166.3	136.1	127.6	127.7

[#] All Temperatures are in °F

TABLE I

INLET TEMPERATURE* PROFILE AT THE TOP, x = 0

Distance from Wall, y, Inches

RUN NO.	.005	.0075	.025	.050	.075	.100	.150	.200	.300	.400	.500
A-1	171.2	---	159.4	149.1	135.3	---	116.3	112.9	85.1	83.4	83.5
A-2	236.3	---	213.6	188.1	179.3	---	145.1	114.6	94.5	86.9	86.8
A-3	318.0	---	300.0	281.3	256.0	---	185.8	157.7	116.3	101.8	99.7
A-4	396.9	---	371.3	342.7	298.8	---	220.2	197.5	118.3	110.7	107.8
X-4	398.9	---	348.6	316.2	---	256.2	179.8	127.7	94.9	87.5	89.1
B-1a	174.6	---	152.9	136.6	---	110.0	---	93.2	92.4	93.0	93.7
B-1b	167.9	---	154.3	140.8	129.0	---	107.9	102.8	100.9	100.7	100.9
B-2a	---	215.2	192.1	156.2	---	151.8	---	92.0	88.5	88.5	88.5
B-2b	224.5	---	199.0	180.8	155.7	---	115.8	107.5	103.9	103.3	103.4
B-3	---	305.4	276.4	239.3	---	173.0	---	100.4	91.8	91.1	91.1
B-4	---	377.8	333.7	293.5	---	216.4	---	107.5	95.0	94.2	93.9
C-1a	---	153.5	137.7	122.7	---	100.7	107.4	93.4	94.6	95.6	95.2
C-1b	163.6	---	148.4	132.5	121.1	---	---	106.1	106.4	106.5	105.5
C-2a	---	209.6	182.7	157.6	---	115.3	110.5	93.3	91.5	92.0	91.5
C-2b	226.8	---	192.2	162.9	143.0	---	---	106.6	104.9	105.3	105.2
C-3a	---	284.7	255.5	212.6	165.4	142.8	113.7	97.3	95.9	96.4	96.8
C-3b	274.0	---	233.8	202.0	---	---	116.3	106.7	104.6	104.8	104.1
C-4	342.1	---	299.5	233.0	194.8	---	---	106.1	102.8	103.3	103.6
D-1a	---	148.2	132.5	115.1	---	97.9	---	95.8	96.9	91.6	97.1
D-1b	157.3	---	145.6	127.3	117.9	---	108.2	108.1	108.7	108.9	109.0
D-2	---	198.0	166.9	140.3	---	106.7	---	99.6	100.0	100.4	100.2
D-3	---	297.0	239.1	192.5	---	122.7	117.7	97.8	97.6	98.3	98.6
D-4	328.1	---	281.1	218.7	167.0	---	---	112.0	110.5	111.1	111.4
E-1	161.8	---	143.1	124.1	113.0	---	107.8	108.4	109.3	109.4	108.8
E-2	223.4	---	185.6	147.3	126.4	---	109.5	109.5	108.4	108.6	108.4
E-3	267.3	---	220.7	165.6	131.4	---	106.7	104.1	103.9	103.9	104.3
E-4	347.7	---	278.3	201.8	145.1	---	107.5	104.3	103.1	102.9	102.6

* All Temperatures are in °F

TABLE III-a

GRADIENT TEMPERATURES, °F

Run No.	Distance from Wall x, inches	Distance from Top, x, inches						
		0	1	3	6	9	11	11¾
A-1	0.005	171.2	199.5	205.0	207.0	203.9	200.9	196.1
	0.025	159.4	188.4	196.9	198.0	192.7	192.9	190.3
	0.050	149.1	179.6	185.4	187.7	179.2	181.8	180.3
	0.075	135.3	166.6	177.2	177.2	167.4	172.3	173.8
A-2	0.005	236.3	273.9	282.7	282.0	284.7	281.0	273.1
	0.025	213.6	254.7	269.8	260.8	271.5	268.5	265.5
	0.050	188.1	234.6	255.1	240.5	253.3	256.8	255.4
	0.075	179.3	210.2	244.3	215.9	237.7	242.6	246.4
A-3	0.005	318.0	376.8	387.9	398.0	397.1	389.3	378.5
	0.025	300.0	360.0	365.9	377.5	380.7	374.6	366.4
	0.050	281.8	335.6	334.2	344.2	362.2	359.9	357.5
	0.075	256.0	316.8	306.1	311.8	339.2	339.6	344.0
A-4	0.005	396.9	468.7	481.0	494.9	496.2	487.5	476.9
	0.025	371.3	447.3	445.2	464.6	476.7	469.3	464.2
	0.050	342.7	417.8	397.2	430.9	451.4	452.4	446.3
	0.075	298.8	391.3	360.9	392.4	426.3	430.8	433.2
X-4	0.005	398.9	467.9	487.4	See Table IV	486.3	475.5	461.3
	0.025	348.6	438.4	459.9		448.4	451.6	440.8
	0.050	316.2	399.8	427.0		404.3	414.3	418.4
	0.100	256.2	324.6	367.0		320.8	359.5	369.4
B-1a	0.005	174.6	195.1	201.0	205.9	204.6	200.9	183.8
	0.025	152.9	180.0	189.2	196.1	197.2	194.2	181.4
	0.050	136.6	163.9	177.1	186.0	186.1	186.4	179.5
	0.100	110.0	135.8	152.9	162.3	169.0	171.0	170.2
B-1b	0.005	167.9	200.5	206.1	209.5	208.3	205.5	201.7
	0.025	154.3	186.3	195.8	200.5	201.9	198.9	196.8
	0.050	140.8	170.6	183.2	191.3	193.4	191.3	191.8
	0.075	129.0	156.9	172.1	180.9	183.4	184.2	185.8
B-2a	0.0075	215.2	274.8	285.2	293.3	291.5	283.7	273.2
	0.025	192.1	255.1	269.4	281.7	278.8	268.8	262.5
	0.050	156.2	211.2	237.1	249.3	250.6	233.2	230.3
	0.100	131.8	179.6	207.9	230.9	225.2	204.4	209.8
B-2b	0.005	224.6	283.4	295.5	303.5	302.2	295.2	286.7
	0.025	199.0	261.7	278.9	288.7	290.3	283.9	277.5
	0.050	180.8	236.1	260.4	272.2	275.1	271.5	265.6
	0.075	155.7	211.9	239.0	254.1	259.6	255.6	251.9

TABLE III-b

GRADIENT TEMPERATURES, °F

Run No.	Distance from Wall y, inches	Distance from Top, x, inches						
		0	1	3	6	9	11	11¾
B-3	0.0075	305.4	363.4	377.6	387.2	380.2	368.0	351.2
	0.025	276.4	337.4	357.0	368.9	357.4	342.9	331.0
	0.050	239.3	304.5	330.4	345.8	328.3	304.8	304.8
	0.100	173.0	242.9	281.5	292.6	266.9	248.0	255.5
B-4	0.0075	377.8	455.6	474.7	484.8	469.7	453.7	437.0
	0.025	333.7	424.1	453.7	463.1	438.3	421.5	419.2
	0.050	293.5	381.6	419.1	432.0	393.8	374.2	377.3
	0.100	216.4						
C-1a	0.0075	153.5	188.8	194.6	199.0	198.4	194.6	189.6
	0.025	137.7	172.3	183.7	188.4	188.8	186.8	186.8
	0.050	122.7	153.9	169.8	176.0	179.2	179.5	180.2
	0.100	100.7	117.6	139.6	147.3	151.7	154.2	160.3
C-1b	0.005	163.6	195.7	202.9	207.3	206.9	203.6	200.6
	0.025	148.4	178.9	190.3	197.3	197.3	196.1	195.4
	0.050	132.5	161.5	176.0	184.6	188.3	186.5	188.4
	0.075	121.1	144.9	161.6	173.0	181.0	176.6	179.2
C-2a	0.0075	209.6	270.8	283.4	291.0	286.8	282.4	277.6
	0.025	182.7	244.9	265.0	273.5	274.4	268.7	267.5
	0.050	157.6	215.0	237.0	252.2	253.7	252.2	250.9
	0.100	115.3	153.1	191.9	204.0	206.8	208.3	214.9
C-2b	0.005	226.8	280.6	294.1	300.8	299.2	291.9	284.7
	0.025	192.2	252.0	271.9	282.0	284.4	278.9	274.2
	0.050	162.9	218.8	245.4	259.3	264.9	261.4	259.7
	0.075	143.0	190.9	221.2	236.8	243.1	239.6	245.4
C-3a	0.0075	284.7	358.0	373.6	382.8	378.5	367.7	345.6
	0.025	255.5	327.1	348.6	363.2	357.7	347.9	337.0
	0.050	212.6	284.2	312.4	325.1	297.7	325.2	314.7
	0.100	142.8	201.4	248.2	263.8	269.6	263.9	265.2
C-3b	0.005	274.0	361.5	383.1	393.9	390.6	380.7	366.4
	0.025	233.8	321.0	350.9	367.9	367.0	359.0	350.4
	0.050	202.0	281.2	322.1	340.0	343.4	336.1	329.4
	0.075	165.4	242.0	287.9	308.2	309.7	306.1	306.1
C-4	0.005	342.1	453.9	480.4	491.9	487.1	470.3	454.6
	0.025	299.5	402.8	440.9	460.5	456.8	445.3	433.6
	0.050	233.0	345.5	396.3	419.9	423.3	406.4	397.6
	0.075	194.8	298.1	359.3	383.2	388.9	370.1	368.6

TABLE III-c

GRADIENT TEMPERATURES, °F

Run No.	Distance from Wall y, inches	Distance from Top, x, inches						
		0	1	3	6	9	11	11 3/4
D-1a	0.0075	148.2	187.4	194.3	198.4	199.1	194.7	193.0
	0.025	132.5	168.8	161.5	186.8	190.7	186.2	187.3
	0.050	115.1	146.9	161.8	171.6	176.3	173.5	178.0
	0.100	97.9	110.4	169.1	137.9	144.8	145.3	153.9
D-1b	0.005	157.3	191.3	199.3	203.8	203.7	199.7	196.3
	0.025	145.6	174.8	186.1	192.9	193.2	191.9	190.0
	0.050	127.3	154.7	169.6	178.8	182.1	181.8	182.8
	0.075	117.9	136.3	153.2	163.5	168.9	168.6	171.4
D-2	0.0075	198.0	267.3	280.3	289.5	287.8	281.4	278.3
	0.025	166.9	237.0	258.1	269.5	271.5	266.2	266.2
	0.050	140.3	201.0	228.1	245.9	250.2	248.5	249.7
	0.100	106.7	133.6	168.4	186.7	195.9	194.0	202.3
D-3	0.0075	297.0	356.7	375.6	381.4	380.5	376.6	352.3
	0.025	239.1	319.9	346.3	357.1	358.3	347.6	338.9
	0.050	192.5	271.3	307.2	321.2	323.4	317.4	310.7
	0.100	122.7	169.4	218.0	242.2	247.3	242.4	257.8
D-4	0.005	328.1	449.2	475.5	487.6	483.0	469.6	452.4
	0.025	281.1	398.8	436.7	455.5	452.4	440.6	430.9
	0.050	218.7	339.4	381.6	413.5	412.8	407.7	404.0
	0.075	167.0	264.8	327.5	354.2	361.6	364.3	368.7
E-1	0.005	161.8	200.7	209.2	212.3	210.4	206.5	204.3
	0.025	143.1	180.4	192.2	197.0	197.5	196.0	196.0
	0.050	124.1	152.6	170.6	177.9	181.0	180.9	184.4
	0.075	113.0	130.6	148.0	158.6	161.7	164.2	170.0
E-2	0.005	223.4	283.5	297.6	300.9	299.4	292.7	286.8
	0.025	185.6	248.8	268.7	277.9	279.1	274.8	273.5
	0.050	147.3	201.9	231.3	243.8	249.0	247.9	252.4
	0.075	126.4	161.3	192.9	208.3	210.8	214.3	220.4
E-3	0.005	267.3	361.6	380.2	387.9	381.3	372.8	361.6
	0.025	220.7	311.6	341.1	356.4	353.3	348.6	243.6
	0.050	165.6	250.0	288.9	312.6	315.2	313.0	315.5
	0.075	131.4	189.7	234.9	259.0	265.4	265.3	278.2
E-4	0.005	347.7	460.7	483.0	493.5	484.1	470.6	454.1
	0.025	278.3	397.0	434.1	451.9	444.3	436.0	429.7
	0.050	201.8	317.6	365.2	394.7	394.6	390.9	396.4
	0.075	145.1	223.1	291.6	317.5	333.0	334.0	345.8

TABLE IV

TEMPERATURE[*]PROFILES RUN x-4

Distance From Wall, y, Inches	Distance from the Top, x, Inches								
	0	1	3	4	5	7	9	11	11 3/4
.005	398.9	467.9	487.4	489.5	490.9	491.2	486.3	475.5	461.3
.025	348.6	438.4	459.9	466.5	461.3	446.0	448.4	451.6	440.8
.050	316.2	399.8	427.0	424.6	425.3	398.5	404.3	414.3	418.4
.100	256.2	324.6	367.0	367.7	352.1	315.3	320.8	359.5	369.4
.150	179.8	247.2	302.4	298.8	293.4	261.3	280.7	300.6	328.9
.200	127.7	175.7	251.0	256.6	256.6	236.0	247.2	273.7	292.3
.300	94.9	100.5	152.4	184.1	204.1	213.4	218.8	246.1	264.1
.400	87.5	91.9	107.8	120.4	153.7	191.7	211.1	223.5	242.4
.500	89.1	90.3	108.6	111.4	128.1	183.0	211.9	221.6	233.8

* All Temperatures are in °F

TABLE V

WALL TEMPERATURES[*]

Run No.	Distance from Top, x, inches					
	1	3	5	7	9	11
A-1	203.1	207.3	209.7	210.9	209.7	206.0
A-2	282.9	290.1	293.6	295.7	293.8	286.9
A-3	384.5	396.3	402.7	406.3	404.0	394.6
A-4	480.1	496.2	505.2	509.9	506.3	493.6
X-4	477.6	494.3	502.2	504.9	500.3	485.2
B-1a	198.2	202.2	204.5	205.9	204.7	200.8
B-1b	206.3	210.3	212.7	214.0	212.9	209.1
B-2a	289.3	296.8	300.6	302.7	300.5	293.0
B-2b	295.7	303.4	307.8	310.1	308.0	300.8
B-3	378.5	389.5	394.9	396.7	392.8	380.8
B-4	475.3	490.9	498.2	500.6	495.1	479.1
C-1a	196.6	200.5	202.6	203.9	202.9	198.9
C-1b	204.4	208.6	211.1	212.5	211.3	207.7
C-2a	286.7	293.9	297.8	299.6	297.3	289.3
C-2b	291.6	299.2	303.5	305.6	303.2	295.6
C-3a	380.2	391.5	397.3	399.7	395.5	384.0
C-3b	384.8	397.3	403.9	406.9	403.4	391.7
C-4	478.7	495.6	504.6	508.1	502.9	486.7
D-1a	198.0	202.3	204.8	206.2	205.1	200.8
D-1b	200.7	204.8	207.3	208.5	207.6	203.8
D-2	288.0	295.6	299.7	301.8	299.5	291.3
D-3	380.0	391.4	397.1	399.9	396.2	383.8
D-4	477.6	494.6	503.6	507.3	502.2	486.0
E-1	208.2	212.7	215.6	217.2	216.2	211.8
E-2	296.2	304.4	309.0	311.2	308.8	300.4
E-3	380.1	392.8	399.4	402.7	398.9	386.4
E-4	477.2	495.0	504.2	508.0	502.3	484.7

[*] All temperatures are in °F.

TABLE VI

FLOW METER DATA

Run No.	Orifice Number	t Av. $^\circ F$	$P_u - P_d$	$P_d - P_b$	P_b
A-1	1	103.0	24.8	0	1037
A-2	1	103.1	25.6	0	1037
A-3	1	111.4	25.5	0	1033
A-4	1	111.5	25.3	0	1028
X-4	1	105.4	60.8	0	1031
B-1a	2	115.8	16.3	0	1040
B-1b	2	118.6	16.0	0	1031
B-2a	2	110.0	15.2	0	1033
B-2b	2	121.1	16.0	0	1036
B-3	2	107.6	15.5	0	1032
B-4	2	111.3	15.9	0	1031
C-1a	2	114.8	35.3	1	1038
C-1b	2	125.0	36.3	1	1031
C-2a	2	110.8	35.3	1	1040
C-2b	2	122.8	36.2	1	1039
C-3a	2	115.7	36.7	1	1033
C-3b	2	121.0	35.9	1	1041
C-4	2	116.2	36.3	1	1032
D-1a	2	117.0	63.5	2	1033
D-1b	2	126.1	64.3	2	1031
D-2	2	116.2	65.1	2	1031
D-3	2	114.7	64.5	2	1030
D-4	2	122.2	64.7	2	1028
E-1	3	125.6	13.2	10	1032
E-2	3	125.2	13.2	10	1029
E-3	3	117.8	13.5	10	1039
E-4	3	115.5	13.5	10	1040

TABLE VII A

OPTICAL DATA

Run No.	L_{opt} Inches	Set#	Film Numbers	Films Used to Evaluate Y_s
A-1	663	G-512	109-114	109-113
A-2	663	G-512	115-118	115-118
A-3	663	G-513	119-122	119-122
A-4	663	G-513	123-126	123,124,126
X-4	663	G-492	87-100	88,91-93,100
B-1a	664	G-405	15-18	16, 18
B-1b	663	G-587	161-165	163,165
B-2a	664	G-405	31-35	32, 34
B-2b	663	G-589	175-178	176,177
B-3	664	G-454	53-56	53-56
B-4	563	G-454	65-68	65-67
C-1a	664	G-405	23-26	24-26
C-1b	663	G-588	166-170	167,168
C-2a	664	G-405	36-40	37-40
C-2b	663	G-589	179-184	181,183
C-3a	664	G-454	57-60	58,59
C-3b	663	G-590	189-192	190,192
C-4	563	G-586	150-154	152,153
D-1a	664	G-405	27-30	28-30
D-1b	663	G-588	171-174	172,174
D-2	664	G-405	47-52	49,50
D-3	563	G-454	61-64	62,63
D-4	563	G-587	155-160	157,160
E-1	663	G-513	127-130	127,130
E-2	663	G-513	131-137	133,136
E-3	563	G-516	138-145	141,145
E-4	563	G-586	146-149	147,149

# Denotes file number of the film in the Photographic Department, University of Delaware, Newark, Delaware

TABLE VII-B

EVALUATION OF LIGHT BEAM DISPLACEMENT* Y_s

Run No.						Distance from top, x, inches											
	0	3/16	1/2	1	2	3	4	5	6	7	8	9	10	11	11 1/2	11 3/4	12
A-1	1.585	1.240	0.985	0.795	0.635	0.610	0.615	0.560	0.670	0.670	0.795	0.975	1.020	1.035	0.985	0.960	–
A-2	1.910	1.395	1.105	0.975	0.810	0.925	1.185	1.345	1.465	1.385	1.285	1.140	0.965	0.855	0.815	0.800	–
A-3	1.835	1.275	1.040	0.955	1.150	1.495	1.760	1.795	1.750	1.550	1.275	1.065	0.950	0.855	0.840	0.035	–
A-4	2.020	1.320	1.125	1.095	1.370	1.685	1.885	1.775	1.620	1.490	1.220	0.980	0.845	0.785	0.795	0.810	–
X-4	2.745	2.055	1.530	1.235	1.075	1.020	1.160	1.555	1.785	2.120	2.205	2.005	1.695	1.425	1.340	1.320	0.540
B-1a	2.120	–	1.625	1.350	1.110	1.010	0.940	–	0.860	–	0.770	–	0.720	–	–	0.660	–
B-1b	2.085	1.705	1.445	1.240	1.020	0.910	0.845	0.770	0.735	0.690	0.655	0.615	0.565	0.555	0.530	0.520	–
B-2a	3.200	2.68	2.125	1.755	1.401	1.221	1.116	1.049	0.984	0.954	0.961	1.003	1.147	1.284	1.341	1.351	0.540
B-2b	3.055	2.630	2.065	1.690	1.370	1.170	1.060	0.990	0.945	0.900	0.870	0.800	0.795	0.665	0.945	0.980	–
B-3	3.605	2.635	2.105	1.735	1.390	1.215	1.110	1.075	1.050	1.055	1.135	1.310	1.615	1.910	1.960	1.920	–
B-4	3.645	2.290	1.740	1.445	1.090	0.965	0.930	0.930	0.965	1.040	1.245	1.540	1.820	1.850	1.720	1.580	–
C-1a	2.620	2.065	1.980	1.660	1.380	1.240	1.135	–	1.185	–	1.090	–	0.989	–	–	0.890	0.540
C-1b	2.415	–	1.715	1.455	1.220	1.085	1.020	0.945	0.915	0.860	0.820	0.770	0.705	0.660	0.605	0.565	–
C-2a	3.93	2.940	2.89	2.36	1.94	1.735	1.620	1.320	1.435	1.180	1.280	1.045	1.180	–	–	0.980	0.980
C-2b	3.420	3.795	2.565	2.160	1.770	1.515	1.395	1.425	1.245	1.245	1.105	1.140	0.995	0.930	0.895	0.825	–
C-3a	4.715	3.740	2.885	2.360	1.920	1.695	1.555	1.490	1.340	1.305	1.195	1.165	1.100	1.075	1.035	0.980	–
C-3b	4.655	3.740	2.970	2.46	1.930	1.715	1.590	1.280	1.390	1.120	1.240	1.060	1.115	1.050	1.035	1.025	–
C-4	4.22	3.22	2.57	2.15	1.760	1.505	1.390	1.280	1.200	1.120	1.070	1.060	1.055	1.090	1.105	1.120	–
D-1e	3.130	2.355	2.405	1.990	1.660	1.470	1.355	1.010	1.185	–	1.090	–	0.980	0.715	–	0.890	0.540
D-1b	2.770	–	1.870	1.570	1.365	1.205	1.130	1.645	1.005	0.950	0.890	0.830	0.770	0.195	0.680	0.620	–
D-2	4.665	3.320	2.865	2.520	2.095	1.870	1.730	1.545	1.545	1.480	1.395	1.340	1.285	1.280	1.165	1.130	–
D-3	4.580	3.905	3.080	2.560	2.020	1.780	1.655	1.545	1.495	1.445	1.400	1.365	1.305	1.230	1.270	1.270	–
D-4	4.620	3.530	2.865	2.430	1.965	1.765	1.615	1.510	1.465	1.430	1.370	1.315	1.255	1.230	1.180	1.165	–
E-1	4.105	2.930	2.385	2.015	1.690	1.545	1.445	1.365	1.315	1.260	1.210	1.145	1.080	1.040	0.975	0.915	–
E-2	5.360	4.145	3.470	2.985	2.545	2.290	2.120	1.965	1.845	1.755	1.670	1.590	1.535	1.455	1.340	1.270	–
E-3	5.715	4.270	3.540	3.035	2.520	2.270	2.080	1.950	1.840	1.745	1.665	1.565	1.490	1.440	1.355	1.255	–
E-4	6.205	5.090	3.630	3.090	2.545	2.240	2.060	1.945	1.850	1.725	1.660	1.605	1.555	1.460	1.445	1.380	–

* Displacements are in inches.

TABLE VIII

TEMPERATURE GRADIENT AT THE WALL, $(\frac{\partial t}{\partial y})_{aT}$,

°F/INCH THERMOCOUPLE DATA

RUN NO.	Distance from the Top, x, Inches							
	0	1	3	6	9	11	11 3/4	12
A-1	512	473	396	422	552	393	320	——
A-2	1264	805	570	840	583	492	327	——
A-3	878	861	858	1192	804	688	477	——
A-4	1313	903	1758	1468	1005	814	627	——
X-4	3280	1506	1350	——	1773	1202	951	——
B-1a	1274	655	529	460	431	306	——	132
B-1b	742	678	444	432	338	298	222	——
B-2a	1320	1124	853	710	700	845	676	——
B-2b	1608	1044	808	700	604	564	468	——
B-3	1672	1363	1168	1015	1225	1408	1158	——
B-4	2874	1768	1252	1228	1790	1830	1320	——
C-1a	1144	733	596	558	506	440	97	——
C-1b	666	818	658	548	496	396	304	——
C-2a	1768	1235	1084	940	825	780	666	——
C-2b	2016	1382	1144	912	758	680	564	——
C-3a	1700	1750	1445	1280	1168	1113	925	——
C-3b	2050	1776	1428	1210	1080	1035	820	——
C-4	2522	2288	1844	1548	1422	1452	1236	——
D-1a	1180	1054	722	656	565	493	324	——
D-1b	666	824	654	542	496	388	310	——
D-2	2150	1522	1145	1147	914	882	797	——
D-3	3794	2015	1700	1420	1332	1176	1043	——
D-4	2414	2518	2134	1654	1666	1358	1068	——
E-1	1060	1014	870	756	660	568	438	——
E-2	1988	1750	1486	1384	1182	1038	766	——
E-3	2410	2440	2124	1676	1548	1402	1118	——
E-4	3968	3170	2680	2208	1480	1462	1224	——

* All Temperatures are in °F.

TABLE IX

TEMPERATURE GRADIENT* AT THE WALL, $\left(\dfrac{\partial t}{\partial y}\right)_{av}$, °F/INCH. OPTICAL DATA

RUN NO.	: Distance from the Top, x, inches																
	0	3/16	1/2	1	2	3	4	5	6	7	8	9	10	11	11 1/2	11 3/4	12
A-1	821	646	513	416	335	325	329	299	360	360	423	520	540	548	518	503	
A-2	1216	892	717	637	536	615	794	899	985	932	867	765	642	563	537	523	281
A-3	1475	1048	864	797	979	1280	1516	1553	1518	1360	1122	931	828	735	715	709	
A-4	2010	1430	1127	1128	1436	1731	2005	1915	1750	1597	1330	1057	917	836	835	845	
X-4	2690	2030	1538	1258	1117	1080	1242	1360	1910	2250	2350	2120	1783	1475	1375	1343	
B-1A	1079		831	696	574	525	489		452		406		376				
B-1B	1092	905	769	663	555	489	457	419	401	377	353	337	305	297	284	343	
B-2A	2030	1730	1392	1157	946	829	751	722	677	656	663	690	779	874	390	278	
B-2B	1968	1720	1372	1130	933	803	745	689	661	630	608	559	550	590	636	896	
B-3	2790	2100	1691	1420	1161	1027	943	920	899	904	972	1114	1343	1560	1590	1552	
B-4	4000	2660	2050	1729	1333	1203	1170	1174	1225	1326	1573	1913	2220	2210	2045	1868	
C-1A	1320	1080	1004	842	714	644	594	510	524	465	475	416	425	355	323	401	
C-1B	1258		907	770	648	580	551		493		443		399			302	285
C-2A	2420	1892	1346	1520	1277	1157	1083	905	971	812	869	717	739	630	602	642	639
C-2B	2180		1658	1413	1140	1030	951	1220	857	1079	759	975	679	898	855	552	
C-3A	3560	2940	2305	1917	1584	1426	1326	1220	1157	1079	1028	934	934	898	855	805	
C-3B	3500	2910	2370	2015	1612	1457	1362	1290	1211	1134	1082	1008	954	885	865	853	
C-4	4510	3610	2960	2540	2140	1968	1740	1622	1537	1433	1370	1349	1315	1336	1335	1459	
D-1A	1570	1214	1225	1020	853	765	711	641	627	509	576	445	530	382	360	460	
D-1B	1407		969	817	719	640	600		539		476	410				329	290
D-2	2850	2100	1842	1638	1394	1260	1177	1127	1059	1017	956	912	872	803	775	745	
D-3	3980	3480	2850	2430	1964	1753	1662	1556	1512	1470	1424	1372	1302	1261	1237	1232	
D-4	4840	3890	3260	2850	2390	2180	2010	1896	1968	1818	1747	1661	1563	1525	1423	1404	
E-1	2080	1527	1250	1067	905	832	785	746	717	690	666	626	589	561	521	490	
E-2	3260	2630	2255	1972	1718	1570	1472	1368	1293	1236	1170	1113	1065	1000	919	861	
E-3	4640	3720	3190	2820	2370	2235	2060	1940	1852	1757	1680	1561	1479	1410	1313	1212	
E-4	5860	5150	3960	3500	2980	2720	2520	2410	2310	2160	2080	2005	1917	1778	1720	1631	

* All Temperatures in °F.

TABLE X

CALCULATED DATA -- DETERMINATION OF q_h, q_T, q_v, N_{Re_l}, N_{Nu_a}, $\emptyset$

Run No.	lb/sec	t_1 °F	t_c °F	q_h BTU/hr	t_w av. °F	k_w av.	$(\partial t/\partial y)_T$ °F/inch	q_t BTU/hr	$(\partial t/\partial y)_{av}$ °F/inch	q_v BTU/hr	t_2-t_1 °F (L=1')	Δt_a °F	N_{Nu_a}	G_h lb/(hr)(sq ft)	$\bar{N}_{Re_l}$	$\emptyset$
A-1	0.00444	93.0	141.5	186	207.6	0.0182	461	143	420	130	35.6	96.8	8.77	250	930	94.7
A-2	0.00451	102.0	193.5	355	290.1	0.0202	684	235	742	255	68.6	153.8	9.73	254	937	86.5
A-3	0.00447	129.7	260.2	497	397.5	0.0227	976	377	1123	434	118.0	208.8	10.87	252	890	76.5
A-4	0.00443	141.8	329.4	718	498.1	0.0249	1242	525	1410	596	163.8	274.4	10.38	249	866	69.1
X-4	0.00710	113.8	262.4	911	493.7	0.0246	1547	655	1555	700	119.9	320.0	10.48	400	1440	111
B-1a	0.00901	95.5	117.8	174	202.4	0.0180	486	150	485	150	20.2	96.7	10.14	507	1870	194
B-1b	0.00874	103.6	124.5	157	210.8	0.0182	438	136	436	136	19.0	97.7	9.05	492	1800	186
B-2a	0.00875	94.5	146.1	390	297.0	0.0203	834	290	834	290	40.3	182.0	9.23	493	1830	167
B-2b	0.00890	108.8	155.6	359	303.9	0.0205	752	263	760	265	36.2	177.0	8.67	501	1820	170
B-3	0.00883	103.3	181.7	597	388.6	0.0225	1232	472	1171	449	61.9	253.3	9.33	497	1820	152
B-4	0.00891	110.2	229.7	919	489.5	0.0246	1519	641	1590	672	91.7	333.4	9.64	502	1820	141
C-1a	0.01326	96.0	111.4	176	200.6	0.0180	572	178	576	178	13.4	97.9	11.88	747	2780	290
C-1b	0.01328	107.7	120.3	145	209.2	0.0182	577	180	525	180	16.4	93.3	11.37	745	2710	284
C-2a	0.01330	95.8	125.3	339	293.9	0.0203	1008	348	1052	363	33.2	181.5	11.72	748	2770	254
C-2b	0.01332	108.7	136.3	318	299.5	0.0204	970	339	927	323	29.4	176.1	10.63	750	2730	254
C-3a	0.01346	102.6	158.4	648	391.3	0.0226	1384	531	1279	490	44.4	266.5	9.70	758	2770	236
C-3b	0.01330	109.9	157.6	547	397.8	0.0228	1312	510	1320	513	47.0	261.4	10.14	749	2720	226
C-4	0.01337	110.8	185.0	857	495.7	0.0248	1731	735	1726	733	66.6	351.6	9.92	753	2730	209
D-1a	0.01779	97.5	107.8	158	202.6	0.0181	697	216	697	216	14.8	97.7	14.40	1002	3700	382
D-1b	0.01773	109.5	118.9	144	205.3	0.0181	571	177	571	177	12.2	89.7	12.87	998	3630	380
D-2	0.01800	101.9	124.9	358	295.8	0.0203	1158	402	1137	394	26.6	180.6	12.73	1013	3720	344
D-3	0.01792	101.3	146.6	704	391.0	0.0226	1607	617	1669	639	43.4	268.0	12.58	1009	3680	308
D-4	0.01790	116.0	169.1	821	495.0	0.0248	1932	820	2004	851	57.8	350.1	11.55	1008	3610	280
E-1	0.0233	109.5	118.2	175	213.5	0.0183	794	249	766	240	12.6	97.7	15.84	1312	4760	494
E-2	0.0233	110.2	126.5	329	304.8	0.0205	1419	495	1393	486	25.4	181.9	15.47	1312	4750	441
E-3	0.0236	106.5	133.3	546	393.1	0.0226	1887	724	1971	756	39.0	267.1	14.91	1329	4340	405
E-4	0.0237	107.1	147.1	820	494.9	0.0248	2329	988	2552	1042	53.4	361.1	13.72	1334	4870	371

TABLE XI

VARIATION OF LOCAL NUSSELT NUMBER WITH LENGTH

Run No.	L Inches	t_2 °F	t_w-t_2 °F	$(\partial t/\partial y)$ °F/inch	$h_x D_0/k_w$ Experimental	Approx. Theory
X-4	0	113.8	348.2	2690	15.31	∞
	1/2	118.6	352.0	1538	8.83	18.07
	1	123.1	354.5	1258	7.19	14.17
	2	130.8	356.4	1117	6.34	11.38
	3	137.0	357.3	1080	6.10	9.92
	4	144.3	354.7	1242	7.07	9.04
	5	152.6	349.6	1665	9.62	8.46
	6	163.9	340.3	1910	11.31	7.87
	7	176.7	328.2	2250	13.84	7.49
	8	190.8	313.0	2350	15.17	7.12
	9	204.0	296.3	2120	14.46	6.86
	10	216.1	277.7	1783	12.99	6.64
	11	226.0	259.2	1475	11.50	6.41
	12	234.3	240.7	1310	10.99	6.25
E-4	0	107.1	356.9	5860	33.31	∞
	1/2	111.0	360.2	3960	22.22	30.68
	1	114.5	362.7	3500	19.51	21.39
	2	120.6	366.6	2980	16.44	16.97
	3	125.5	369.5	2720	14.89	14.82
	4	130.3	369.9	2520	13.78	13.49
	5	134.9	369.3	2410	13.19	12.48
	6	139.1	368.1	2310	12.67	11.77
	7	143.1	364.9	2160	11.98	11.19
	8	146.9	360.1	2080	11.66	10.69
	9	150.6	351.7	-	11.51	10.28
	10	154.2	340.9	1917	11.35	9.93
	11	157.5	327.2	1778	10.99	9.61
	12	160.5	309.5	1560	10.18	9.33

TABLE XII

HEAT-TRANSFER RELATIONS
FOR PARABOLIC VELOCITY DISTRIBUTION
AND CONSTANT WALL TEMPERATURE

$\phi = \dfrac{cGD^2}{kL}$	Round Ducts			Flat Ducts		
	$\dfrac{h_1 D}{k}$	$\dfrac{h_a D}{k}$	$\dfrac{h_L D}{k}$	$\dfrac{h_1 D_e}{k}$	$\dfrac{h_a D_e}{k}$	$\dfrac{h_L D_e}{k}$
1	0.25	0.50	3.68	0.25	0.50	7.60
2	0.50	0.99	3.76	0.50	1.00	7.60
3	0.75	1.48	3.81	0.75	1.50	7.60
4	0.98	1.92	3.86	1.00	2.00	7.60
5	1.20	2.29	3.91	1.24	2.48	7.62
6	1.39	2.60	3.96	1.49	2.95	7.65
7	1.57	2.86	4.01	1.73	3.42	7.69
8	1.74	3.07	4.06	1.96	3.85	7.74
9	1.89	3.25	4.11	2.18	4.23	7.80
10	2.03	3.41	4.16	2.39	4.58	7.86
12	2.27	3.66	4.26	2.78	5.18	7.92
15	2.60	3.96	4.41	3.30	5.89	7.98
20	3.05	4.38	4.70	4.00	6.67	8.05
25	3.43	4.72	4.97	4.55	7.16	8.15
30	3.76	5.02	5.22	5.00	7.50	8.24
40	4.33	5.52	5.67	5.74	8.04	8.52
60	5.22	6.32	6.48	6.73	8.67	8.93
10	6.23	7.24	7.30	7.87	9.54	9.67
130	7.27	8.18	8.23	8.97	10.4	10.5
200	8.63	9.45	9.45	10.4	11.6	11.6
300	10.1	10.8	10.8	12.0	13.1	13.1
400	11.2	11.9	11.9	13.4	14.4	14.4
600	13.0	13.6	13.6	15.4	16.2	16.2
1000	15.6	16.1	16.1	18.8	19.5	19.5
2000	19.9	20.3	20.3	23.3	23.9	23.9
3000	22.9	23.3	23.3	20.4	26.9	26.9
4000	25.3	25.6	25.6	28.9	29.3	29.3
6000	29.0	29.3	29.3	33.1	33.5	33.5
10000	34.6	34.8	34.8	39.6	39.9	39.9
20000	43.6	43.8	43.8	50.0	50.2	50.2
30000	50.0	50.2	50.2	57.0	57.2	57.2
40000	55.1	55.2	55.2	62.6	62.8	62.8

TABLE XIII

THERMOCOUPLE CALIBRATION

Temp. °F	Iron-Constantan		Copper-Constantan	
	Average Deviation from Standard °F	Maximum Deviation from Average Deviation °F	Average Deviation from Standard °F	Maximum Deviation from Average Deviation °F
76.8	-0.5	0.36	-0.1	0.56
105.2	-1.0	0.58	-0.1	0.53
124.6	-0.9	0.53	0.1	0.54
147.4	-1.3	0.58	0.0	0.62
168.2	-1.6	0.56	0.1	0.70
190.7	-2.2	0.61	0.1	0.70
212.3	-2.2	0.64	0.1	0.70
235.4	-2.4	0.68	0.2	0.70
254.0	-2.5	0.78	0.1	0.78
274.9	-2.8	0.81	0.3	0.86
293.6	-3.1	0.89	0.5	0.86
313.6	-3.5	0.92	0.5	0.89
333.2	-3.3	0.94	0.6	0.91
355.5	-3.7		0.8	
375.7	-3.5			

TABLE XIV

ORIFICE CALIBRATION

Orifice	D_o ft.	N_{Re_o}	C_o
1	0.02475	8,200	0.621
		11,590	0.613
		15,220	0.607
		18,100	0.614
		22,060	0.605
		25,900	0.604
		30,150	0.606
		33,100	0.605
		36,150	0.603
2	0.03935	18,700	0.613
		23,800	0.609
		29,550	0.606
		34,130	0.601
		40,100	0.604
		45,400	0.604
		51,650	0.604
		55,150	0.603
3	0.0656	30,660	0.625
		40,900	0.628
		49,200	0.625
		59,500	0.625
		69,400	0.625

$$D_p = 0.1600 \text{ ft.}$$

TABLE XV

CENTER-LINE CORE TEMPERATURE,* °F

RUN NO.	Distance from the top, x, inches						
	0	1	3	6	9	11	11 3/4
A-1	83.5	83.5	90.6	100.9	124.8	130.9	134.6
A-2	80.8	90.5	122.6	140.1	163.4	176.0	177.6
A-3	99.7	104.3	138.1	189.5	220.8	238.6	240.1
A-4	107.8	120.6	175.8	220.7	280.7	293.4	302.5
X-4	89.1	90.3	108.6	——	211.9	221.6	233.8
B-1b	100.9	101.3	102.0	103.6	106.2	109.9	109.3
B-2b	103.4	103.7	104.5	107.8	118.2	124.6	127.1
B-3	91.1	91.6	93.6	103.2	126.4	151.7	159.2
B-4	93.9	94.7	96.8	111.7	171.4	192.6	201.3
C-1b	106.5	106.6	106.7	107.3	109.1	109.9	110.5
C-2b	105.3	105.6	105.8	108.0	110.9	115.4	116.3
C-3a	96.8	97.1	98.0	102.3	114.4	121.7	123.4
C-3b	104.1	104.3	105.1	108.6	116.9	124.6	126.0
C-4	103.6	104.5	105.8	110.7	122.6	140.5	143.1
D-1b	109.0	108.9	109.0	109.4	110.6	111.4	112.2
D-2	100.2	100.2	100.3	102.0	104.9	107.4	109.4
D-3	98.5	98.6	99.1	102.4	108.7	115.9	118.9
D-4	111.4	112.3	113.3	118.2	126.0	135.3	137.5
E-1	108.8	108.6	108.6	109.0	110.8	111.8	112.5
E-2	108.4	108.2	108.8	110.6	113.6	116.8	117.2
E-3	104.3	104.3	104.8	107.4	112.2	116.7	118.4
E-4	102.6	103.3	104.7	108.2	115.6	121.9	125.9

* All Temperatures are in °F.

THERMOCOUPLE

THERMOCOUPLE

THERMOCOUPLE

ORIFICE
METER

COOLING
WATER

COOLING
WATER

THERMOCOUPLE

THERMOCOUPLE

TRAVELING
THERMOCOUPLE

STRIP
HEATERS

INSULATION
OUTLINE

CENTRIFUGAL
BLOWER

THERMOCOUPLE

THERMOCOUPLE
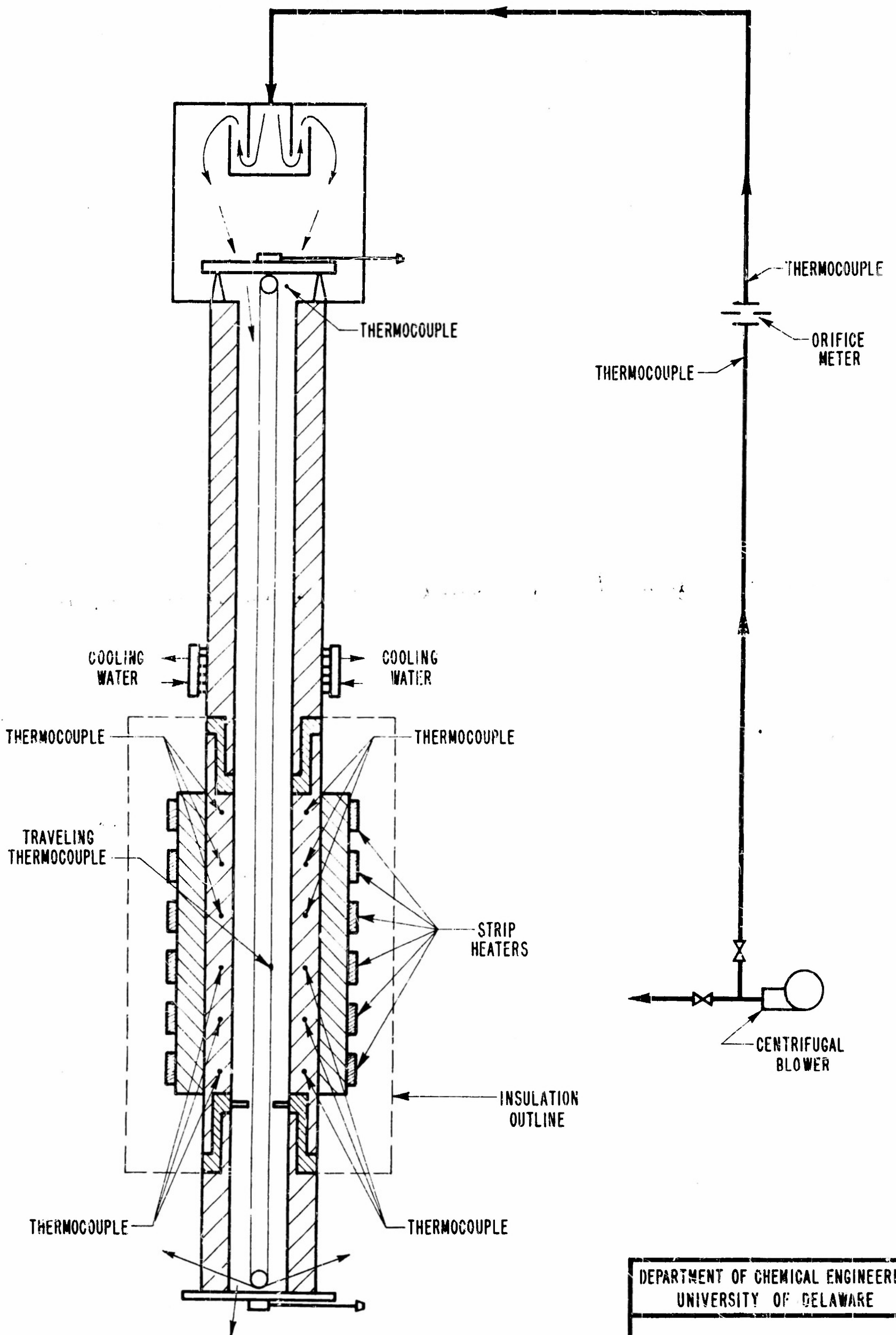
DEPARTMENT OF CHEMICAL ENGINEERING
UNIVERSITY OF DELAWARE

FLOW DIAGRAM

| DATE 8-1-52 | BY R.J.H. | FIG. NO. 1 |

SECTION B-B

SECTION A-A
(SIDE ELEVATION)

FRONT ELEVATION

DEPARTMENT OF CHEMICAL ENGINEERING
UNIVERSITY OF DELAWARE

FUNDAMENTAL DETAILS
OF TEST UNIT

DATE 8-18-52 | BY R J H | FIG 2

CONSTANT VOLTAGE TRANSFORMERS

110 VOLT INPUT

110 VOLT INPUT

FUSED LINE DISCONNECT SWITCHES

VARIABLE VOLTAGE TRANSFORMERS

DOUBLE POLE, DOUBLE THROW MAGNETIC SWITCHES

WATTMETER

BANK 1
BANK 2
BANK 3
BANK 4

TO LOAD
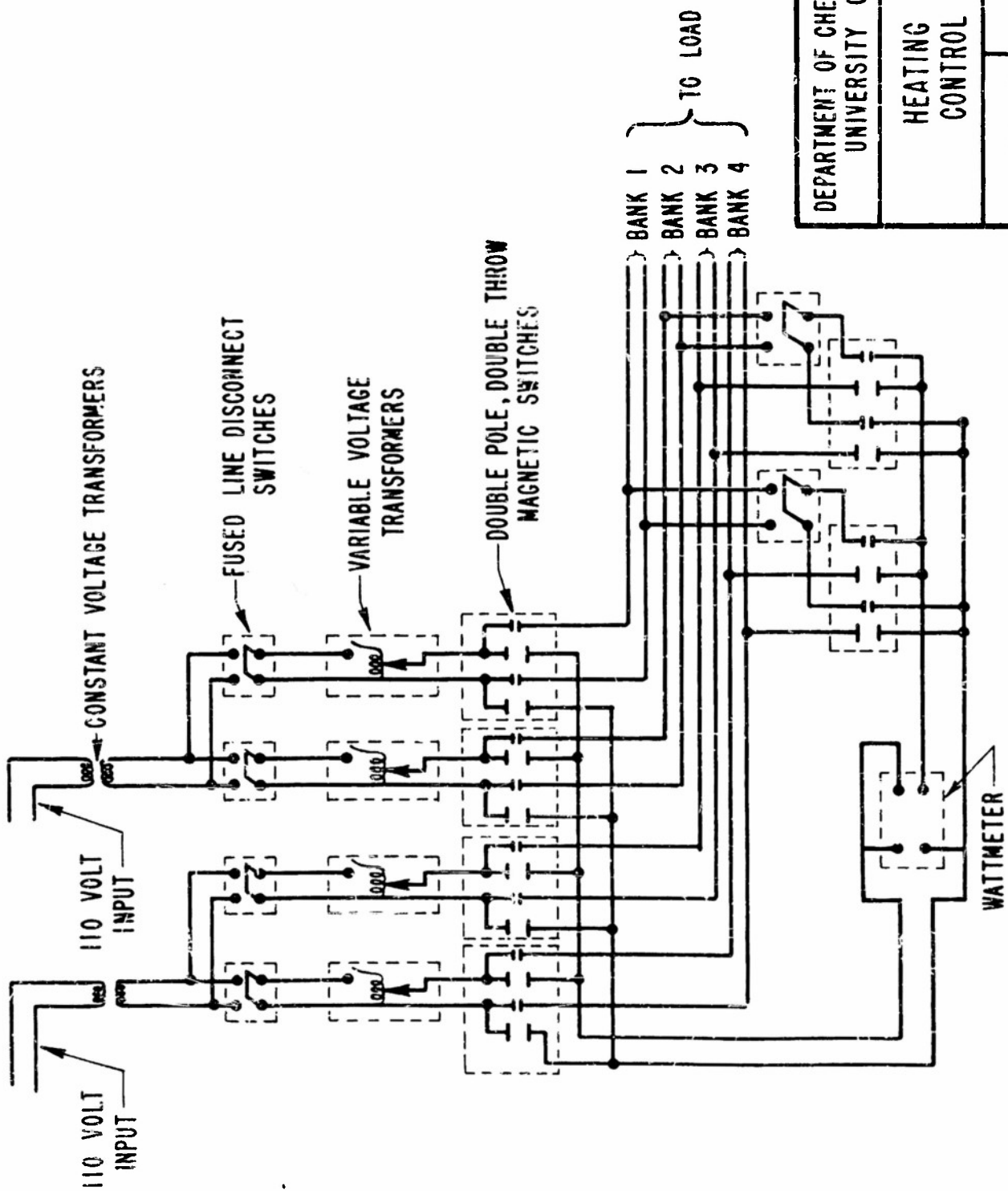
DEPARTMENT OF CHEMICAL ENGINEERING
UNIVERSITY OF DELAWARE

HEATING ELEMENT
CONTROL SYSTEM

DATE 7-20-52 | BY R.J.H. | FIG. NO. 3

ARC LAMP

PIN HOLE

SHUTTER

LENS

PARABOLIC MIRROR

PARALLEL LIGHT

PLANE FRONT-SURFACE MIRROR

TEST UNIT

12.6'

PLANE FRONT-SURFACE MIRROR

24.2'

17.9' OR 9.1'

PHOTOGRAPIC PLATE
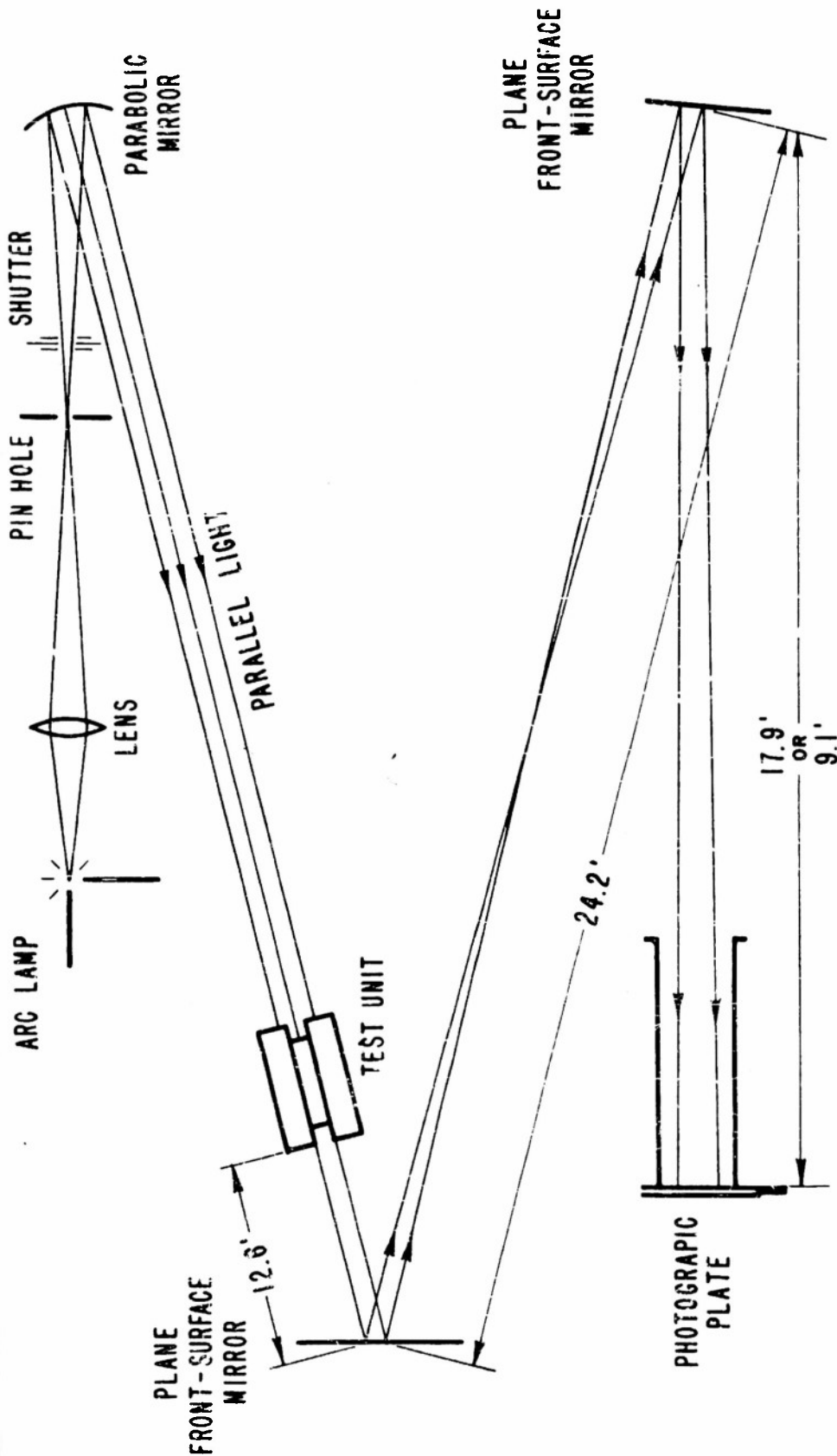
DEPARTMENT OF CHEMICAL ENGINEERING
UNIVERSITY OF DELAWARE

OPTICAL ARRANGEMENT

DATE 7-20-52 | BY R.J.H. | FIG. NO. 4
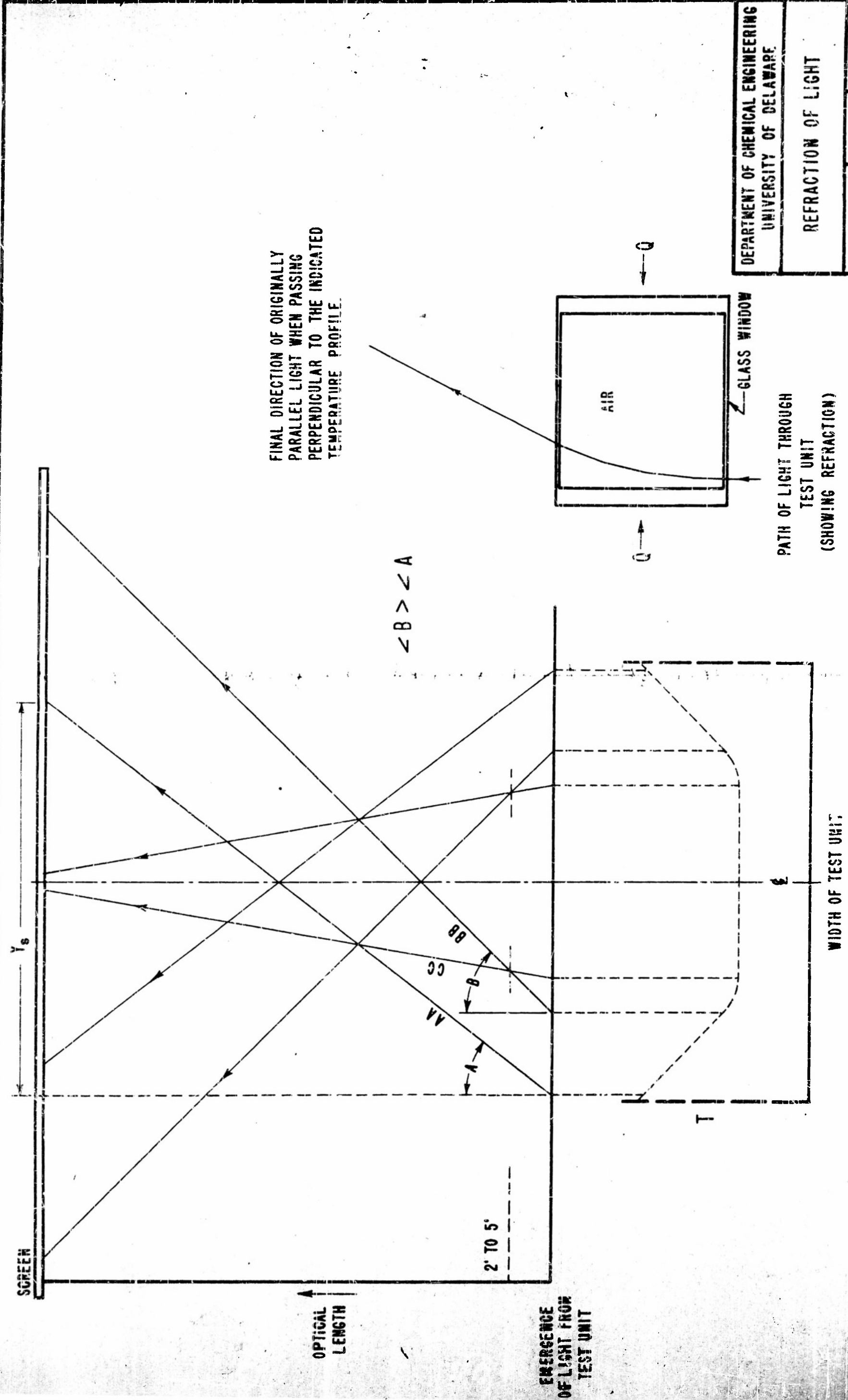
FINAL DIRECTION OF ORIGINALLY PARALLEL LIGHT WHEN PASSING PERPENDICULAR TO THE INDICATED TEMPERATURE PROFILE.

∠B > ∠A

AIR

GLASS WINDOW

PATH OF LIGHT THROUGH TEST UNIT
(SHOWING REFRACTION)

WIDTH OF TEST UNIT

BB

CC

AA

B

A

OPTICAL LENGTH

SCREEN

Ys

2' TO 5'

T

EMERGENCE OF LIGHT FROM TEST UNIT

COMPOSITE PHOTOGRAPHS

RUN E-4   RUN B-1B
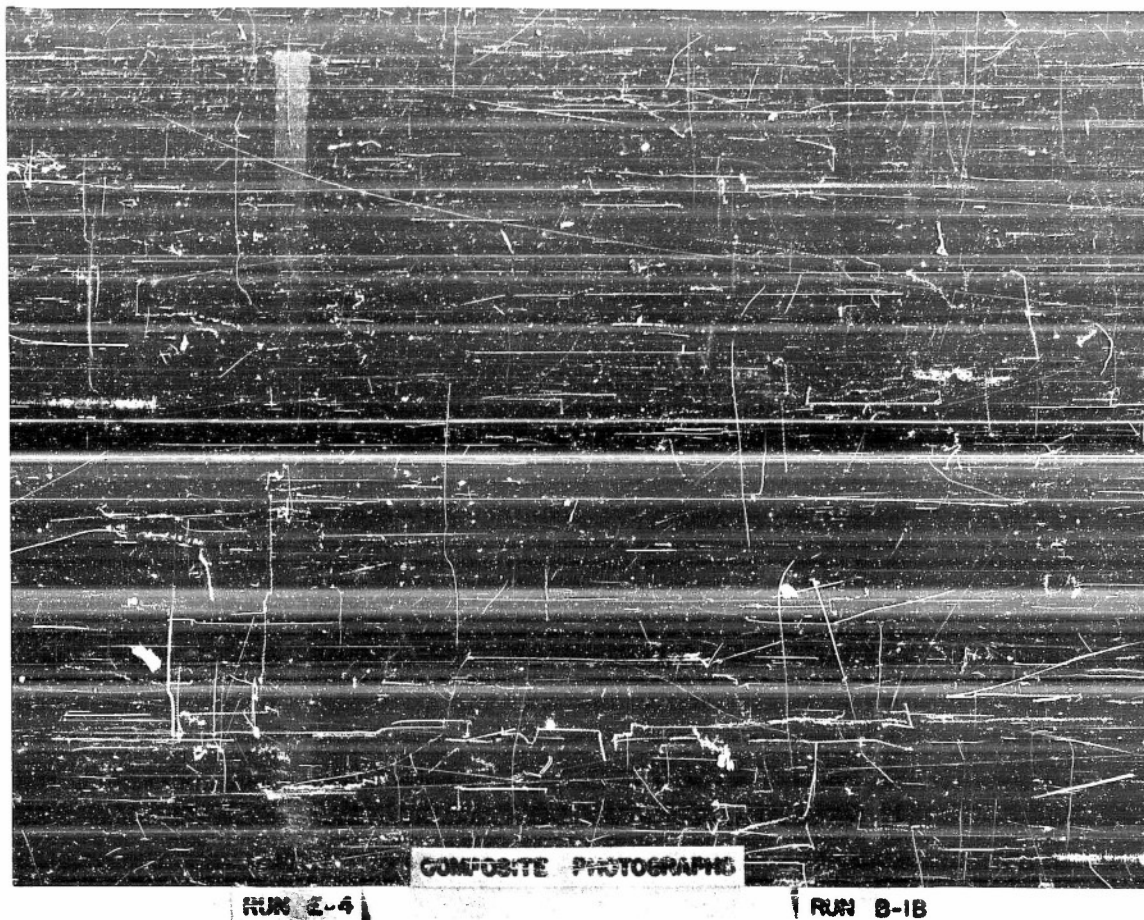
Figure 6. Composite shadowgraphs of runs in which
the upward buoyant effect is not noticeable.

WITHOUT STOP

WITH STOP

COMPOSITE
PHOTOGRAPHS
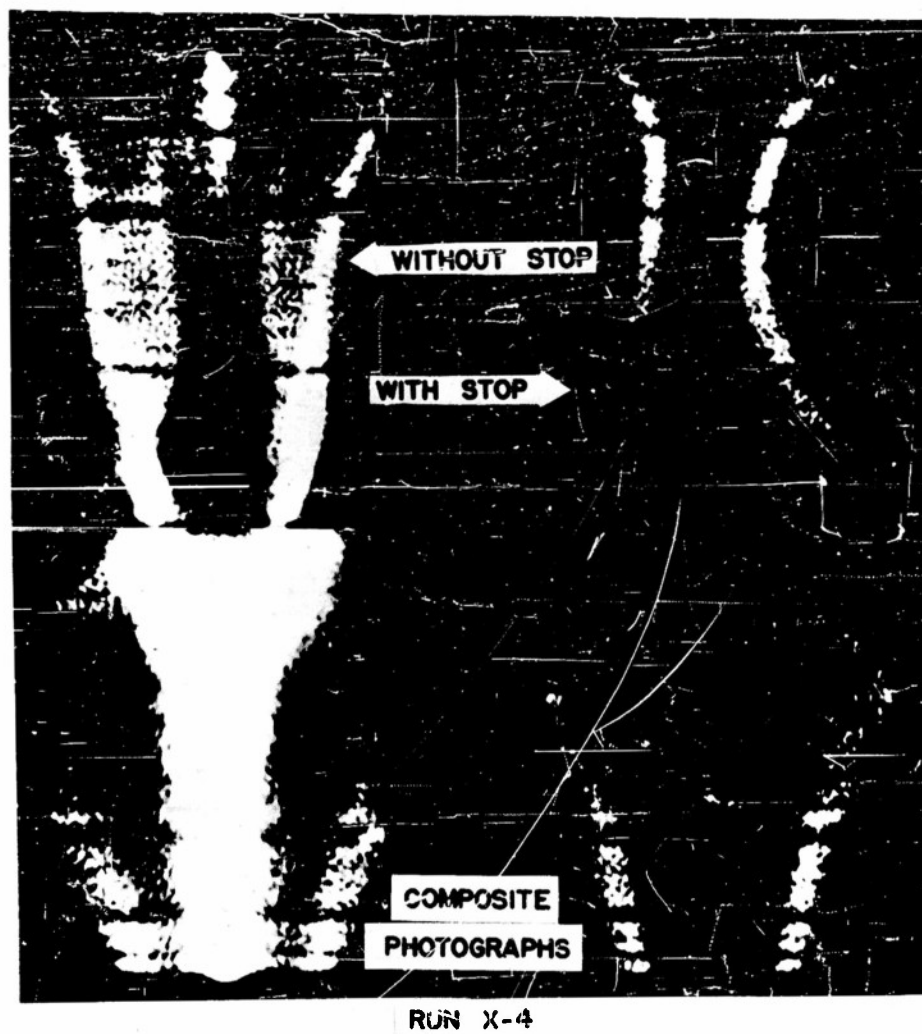
RUN X-4

Figure 7. Composite shadowgraphs of Run X-4 in
which the upward buoyant effect is noticable.

Figure 8. Short-range shadowgraphs of Run X-4.
Lowest horizontal bar on the upper heating
section photo (left) is at the same position
in the test unit as the highest bar on the
lower heating section photo (right).
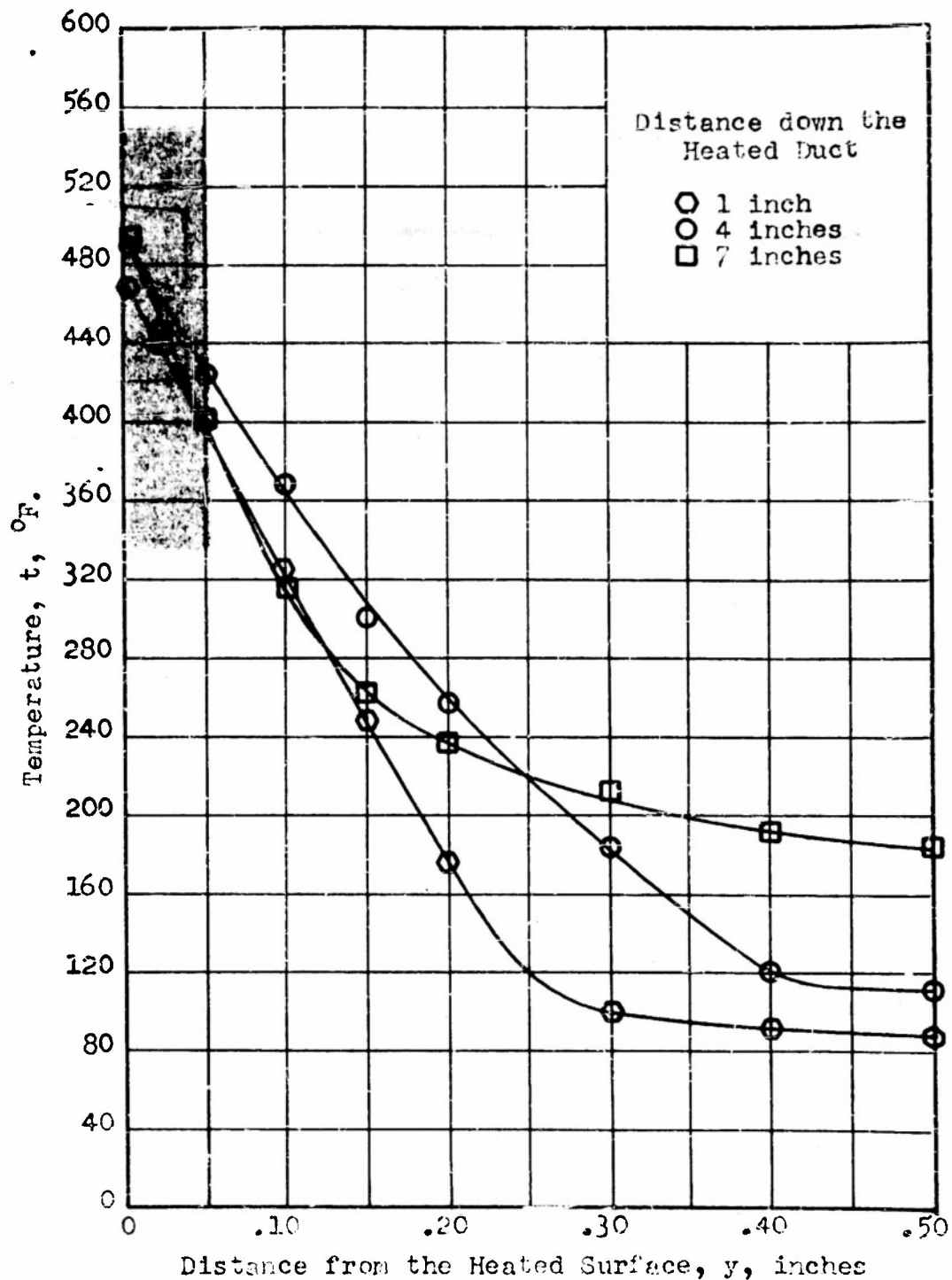
Figure 9. Temperature versus Distance from the Heated Surface at Various Distances Down the Heated Duct in Run X-4.
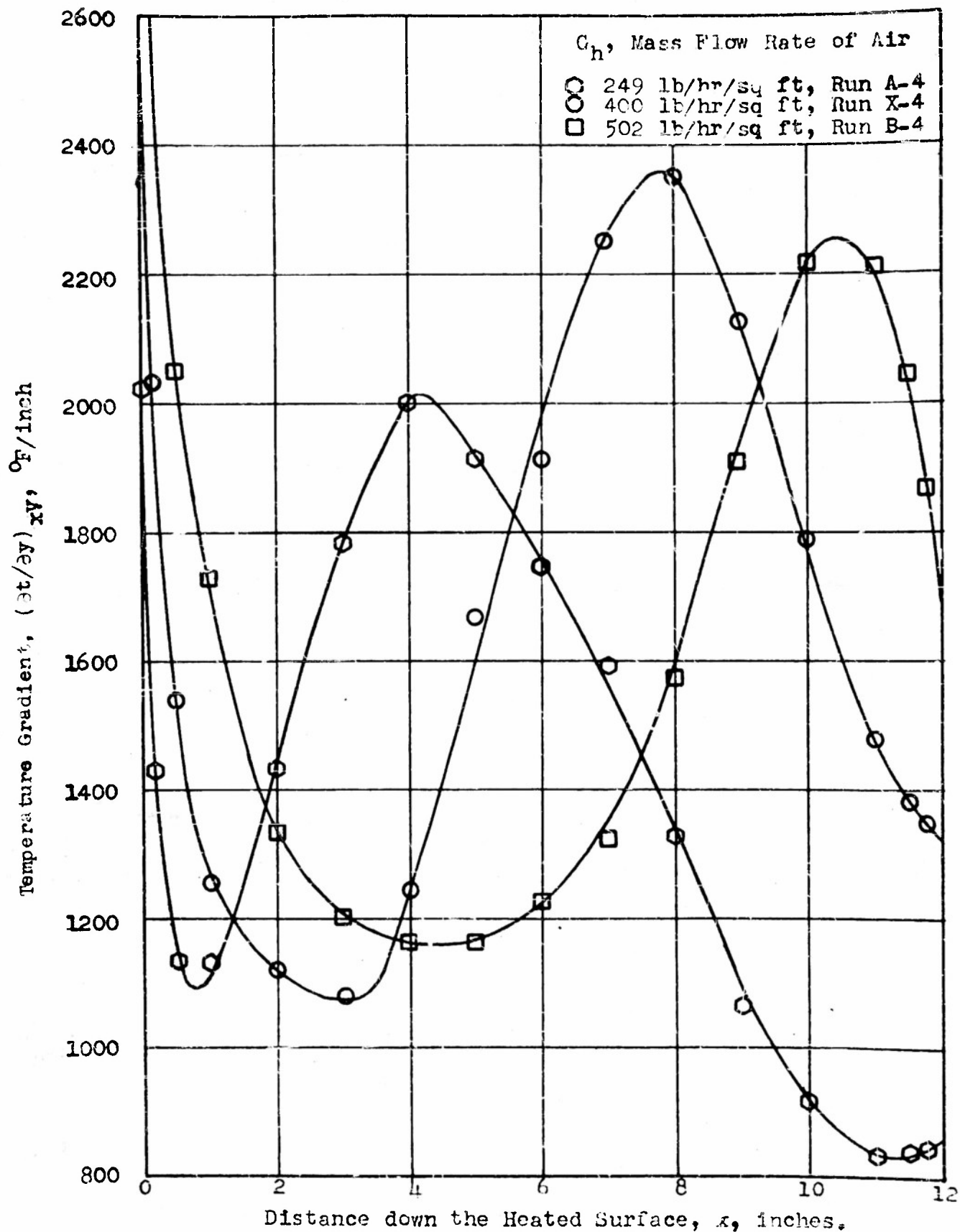
Figure 19. Variation of Air Temperature Gradient at the Wall versus Distance down the Heated Surface at Various Flow Rates and Constant Average Wall Temperature
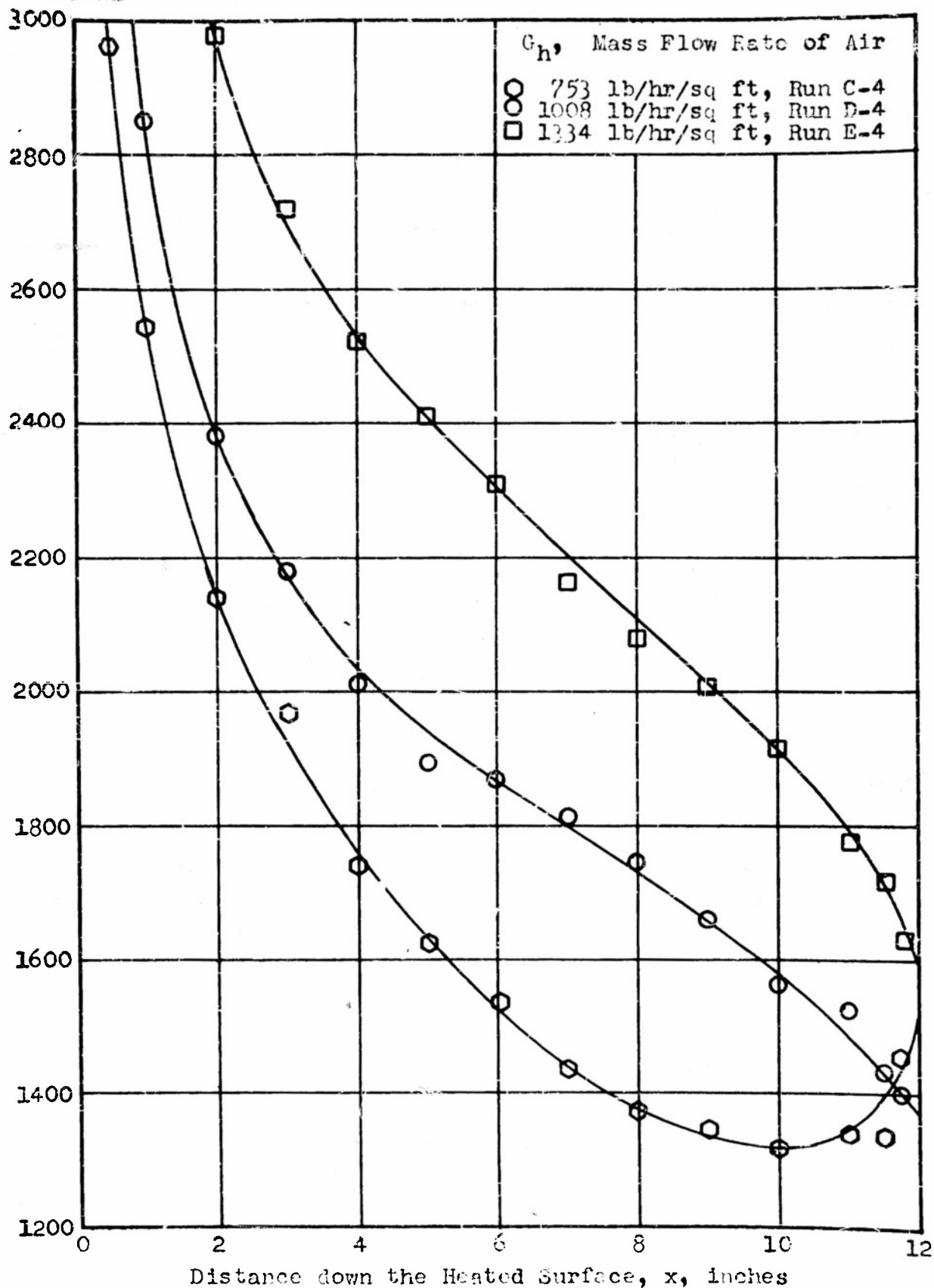
Figure 11. Variation of Air Temperature Gradient at the
Wall versus Distance down the Heated Surface at Various
Flow Rates and Constant Average Wall Temperatures.
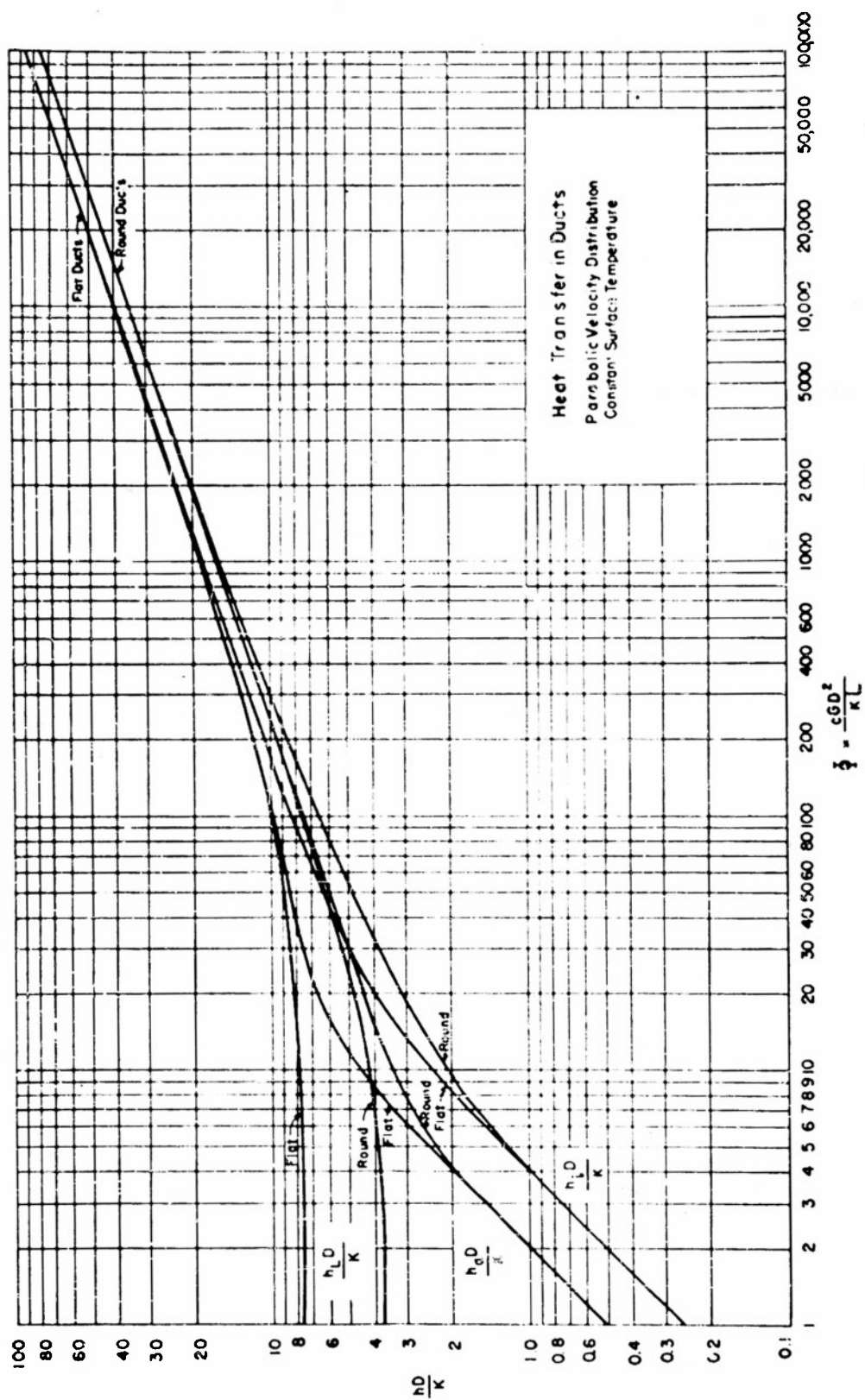
THEORETICAL HEAT-TRANSFER CORRELATION FOR LAMINAR FLOW IN BOTH FLAT AND ROUND DUCTS; RESULTS SHOWN ON LOGARITHMIC-MEAN, ARITHMETIC-MEAN, AND INLET-TEMPERATURE-DIFFERENCE BASES
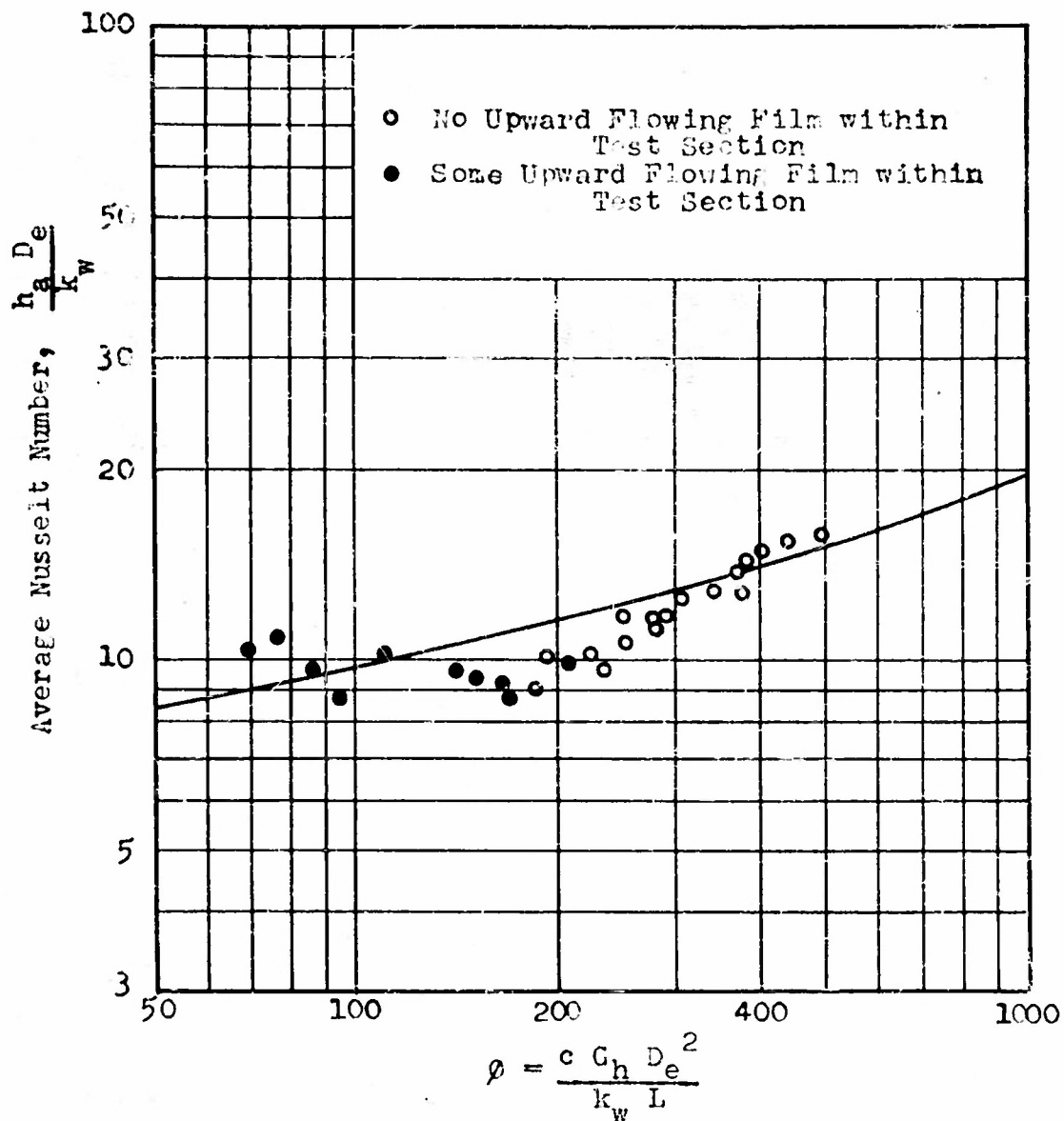
Figure 13. Comparison of Experimental Data of the One Foot Heated Length of Duct with the Theoretical Expression (solid line).
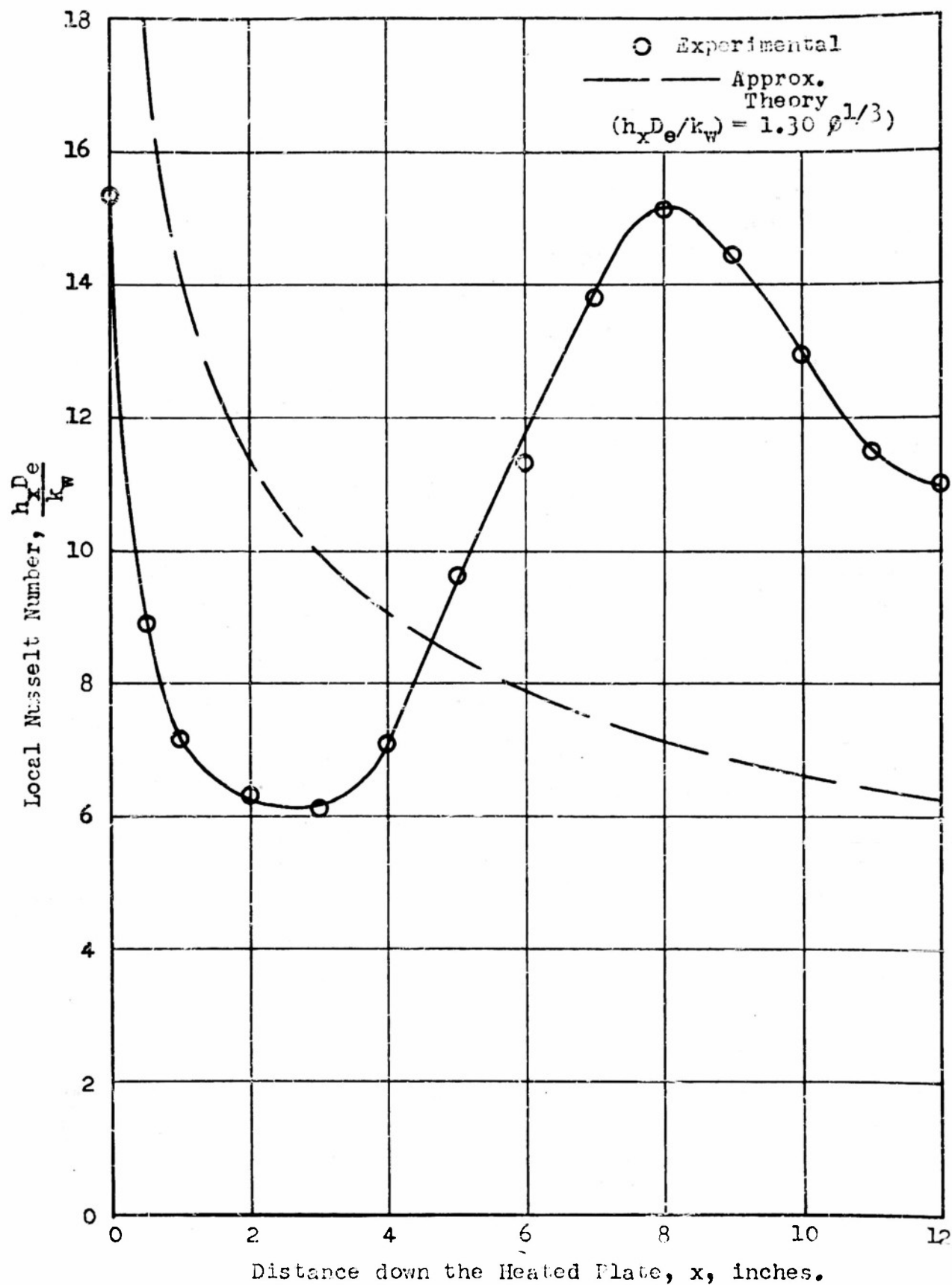
Figure 14. Comparison of Local Nusselt Number with Distance down the Heated Surface for Run X-4.
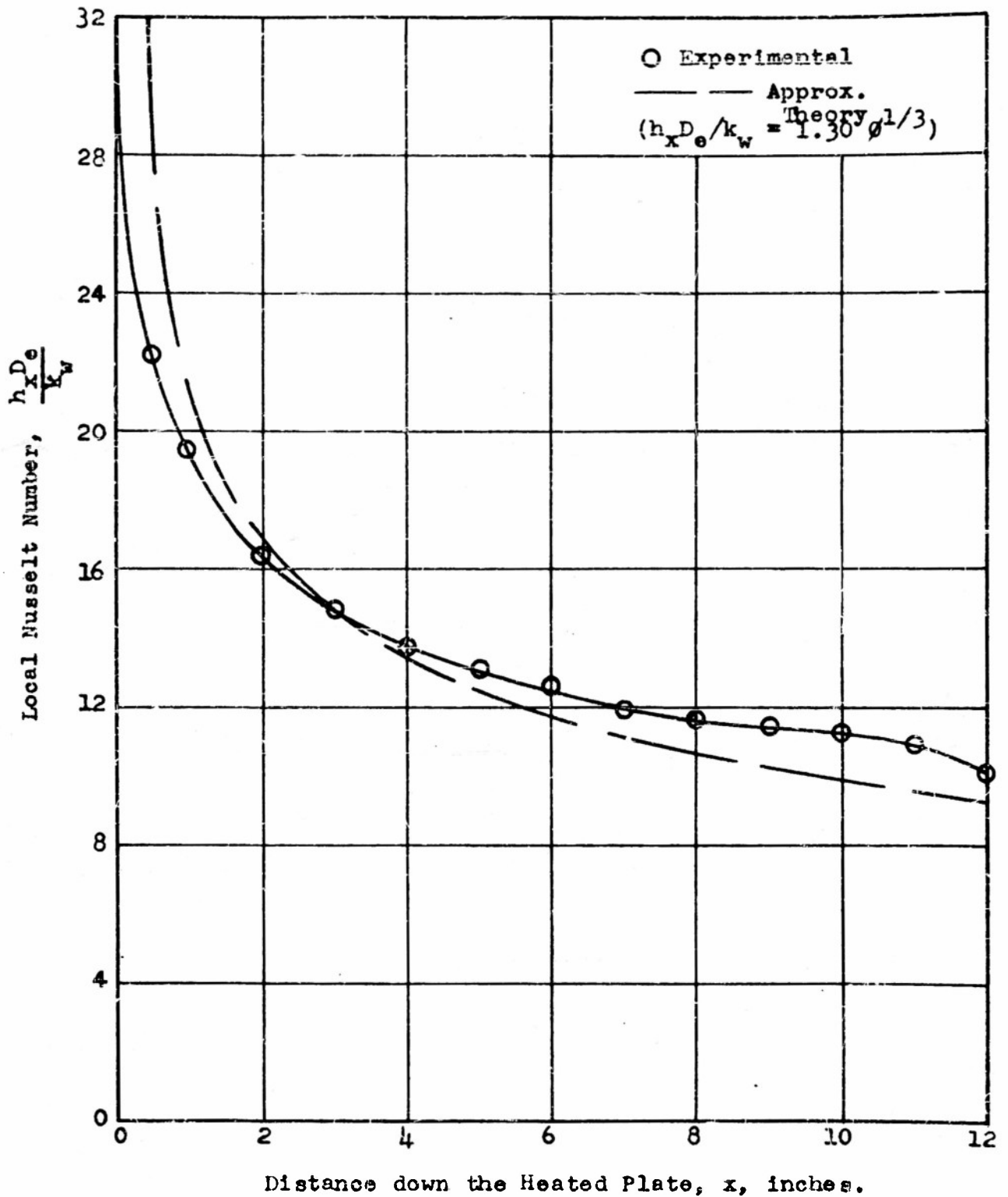
Figure 15. Comparison of Local Nusselt Number with Distance down the Heated Surface for Run E-4.
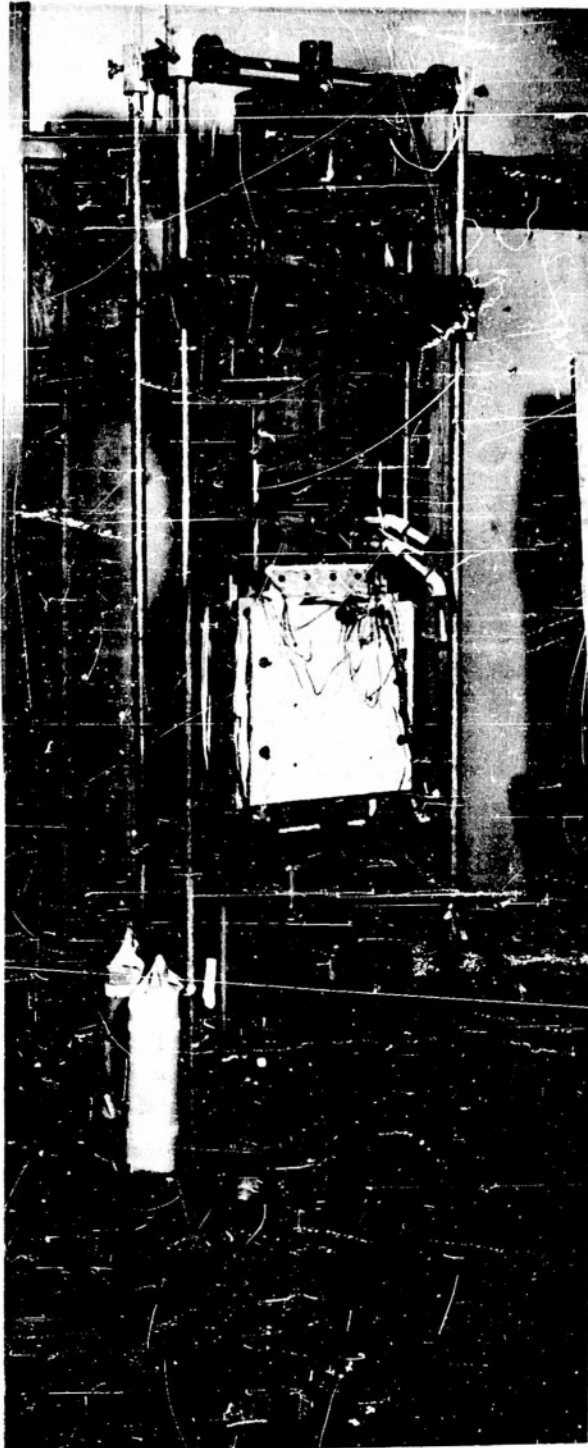
Figure 16. Complete test unit.

Figure 18. Heated section of test unit without heating elements.
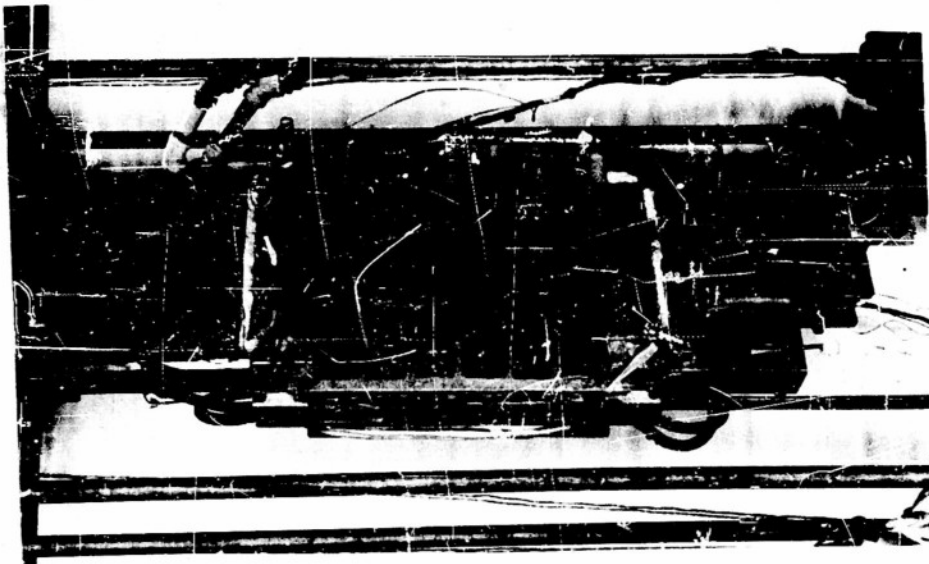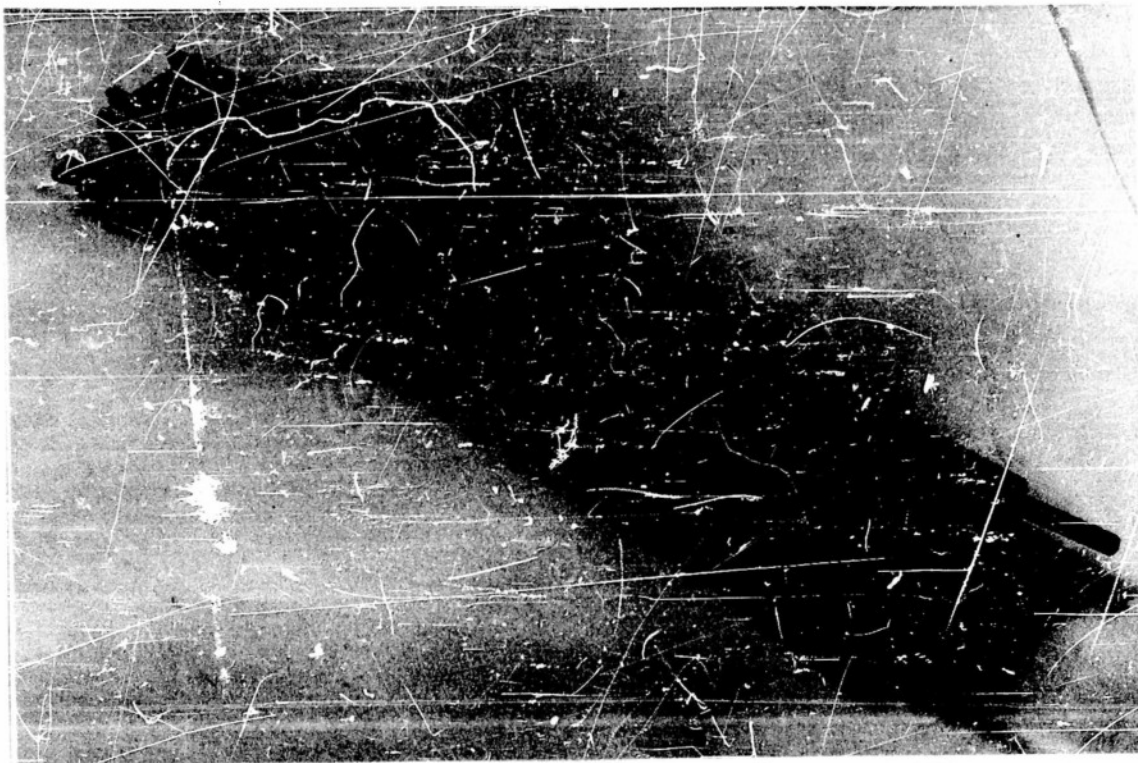

Figure 17. Heated section of test unit showing heating elements.

Figure 19. Window frame showing flush
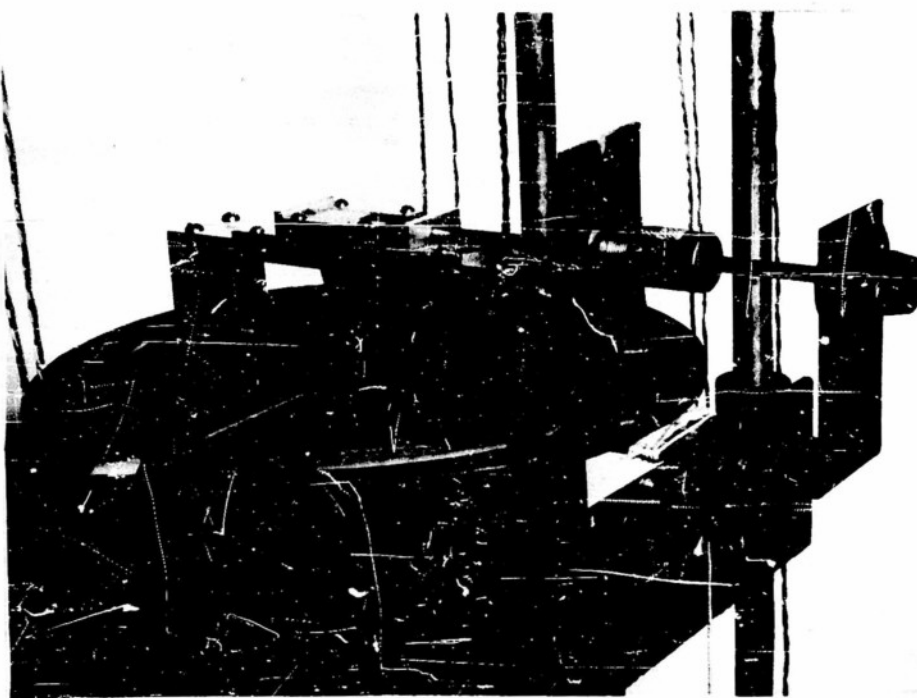nature of glass with the end wall.
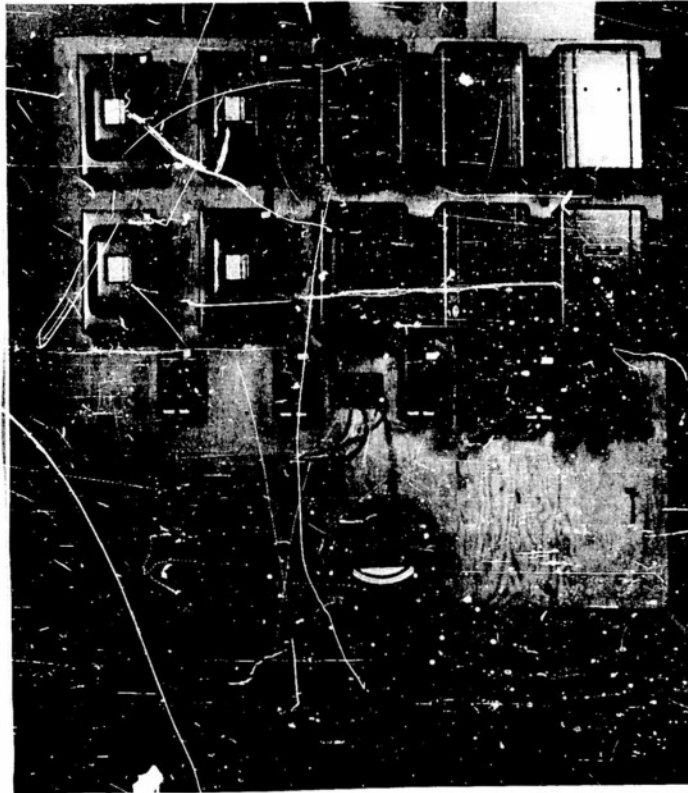

Figure 20. Top Traverse Mechanism

Figure 21. Control Board